Research Square

Preprints are preliminary reports that have not undergone peer review.
They should not be considered conclusive, used to inform clinical practice,
or referenced by the media as validated information.

Comparative Physiological and Biochemical Responses of Chlorella sorokiniana (PX796505) and Tetradesmus wisconsinensis (PX454383) under Arsenic Stress: Mechanistic Insights into a Sustainable Dual-Application Approach

Chandan Mandal

chandanmandal455@gmail.com

Vidyasagar University

Amal Kumar Mondal

Vidyasagar University

Samir Mandi

Vidyasagar University

Prashant Swapnil

Central University of Punjab

Research Article

Keywords: Chlorella sorokiniana, Tetradesmus wisconsinensis, Arsenic stress, Phycoremediation, Stress-induced lipid accumulation, Circular bioeconomy

Posted Date: February 10th, 2026

DOI: https://doi.org/10.21203/rs.3.rs-8603581/v1

License: This work is licensed under a Creative Commons Attribution 4.0 International License.
Read Full License

Additional Declarations: No competing interests reported.

Comparative Physiological and Biochemical Responses of *Chlorella sorokiniana* (PX796505) and *Tetradesmus wisconsinensis* (PX454383) under Arsenic Stress: Mechanistic Insights into a Sustainable Dual-Application Approach

Chandan Mandal[1*], Amal Kumar Mondal[1*], Samir Mandi[1] and Prashant Swapnil[2]

1. Plant Taxonomy, Biosystematics and Molecular Taxonomy Laboratory, UGC-DRS-SAP and DBT-BOOST WB Supported Department, Department of Botany and Forestry, Vidyasagar University, Midnapore-721102, West Bengal, India.

2. School of Basic Science, Department of Botany, Central University of Punjab, Bathinda-151401, India.

*Email: chandanmandal455@gmail.com, akmondal@mail.vidyasagar.ac.in

Abstract

Arsenic contamination of aquatic ecosystems constitutes one of the major environmental and public health concerns. Therefore, remediation strategies should be sustainable and low cost. The present study comprises a comparative physiological and biochemical evaluation of *Chlorella sorokiniana* (PX796505) and *Tetradesmus wisconsinensis* (PX454383) under arsenite [As(III)] and arsenate [As(V)] stress, with special emphasis on arsenic removal efficiency and bioenergy potential. Microalgal cultures were treated with arsenic concentrations ranging from 0 to 125 mg L^{-1} for 28 days. Growth performance, chlorophyll content, biochemical composition (proteins, carbohydrates, and lipids), ultrastructural alterations, and arsenic removal efficiency were systematically evaluated. Both microalgae exhibited clear species- and speciation-dependent responses. Arsenite caused stronger early toxicity than arsenate. This resulted in pronounced growth inhibition and chlorophyll depletion, particularly in *C. sorokiniana*. Despite this initial sensitivity, *C. sorokiniana* expressed higher tolerance under environmentally relevant arsenate concentrations and reached higher arsenic removal efficiency, revealing its suitability for long-term bioremediation purposes. On the other hand, *T. wisconsinensis* had exhibited significant lipid amassment upon exposure to both arsenic species, which reflected a stress-induced carbon reallocation toward lipid biosynthesis, improving its biofuel aptitude. Ultrastructural analysis revealed active arsenic-induced cellular remodeling in both species, endorsing the activation of

adaptive and detoxification mechanisms. In general, this study demonstrated that both studied microalgae could serve a dual functional role: *C. sorokiniana* as an efficient arsenic scavenger and *T. wisconsinensis* for value-added biomass toward bioenergy. This work provides an important mechanistic and application-oriented framework that merges arsenic bioremediation with renewable bioresource production.

Keywords *Chlorella sorokiniana*, *Tetradesmus wisconsinensis*, Arsenic stress, Phycoremediation, Stress-induced lipid accumulation, Circular bioeconomy

Introduction

Arsenic (As) contamination is considered one of the most serious global environmental and public health challenges, particularly in South and Southeast Asia (Shaji et al. 2020). Elevated levels of As are present in soils and aquatic systems due to both natural geogenic processes and anthropogenic processes, including mining, applying pesticides, smelting, and improper disposal of industrial waste (Xing et al. 2024). Arsenic contamination is still an issue. Once in the environment, arsenic will undergo numerous redox transformations and exist mainly as inorganic arsenite [As (III)] and arsenate [As (V)]. These two species vary significantly in mobility, bioavailability, and toxicity (Yamamura and Amachi 2014). Arsenite is more soluble and has high toxicity owing to its high affinity for sulfhydryl groups in proteins over arsenate, and it either enters the cells or competes with phosphate (Bashir 2020). Chronic exposure to As from water and food web systems causes severe health impacts, such as carcinogenesis, cardiovascular diseases, and neurodevelopmental disorders, thereby requiring rapid and sustainable remedial actions (Rahman et al. 2009; Tyler and Allan 2014).

Many traditional techniques used in the removal of arsenic, including chemical precipitation, ion exchange, coagulation and flocculation, adsorbents, and membrane filtration, have high operating costs and require large amounts of energy to operate; as such, these techniques often produce additional toxic sludge as waste material. In addition, these techniques often are ineffective with low metal concentrations and are less practical for larger-scale and rural applications (Mohanty 2017). Therefore, because of these issues, new environmentally-friendly, cost-effective, sustainable methods for removing arsenic have gained greater popularity. As such, research is now being focused on using biological systems, such as microalgae, to remediate

heavy metals and metalloids through their unique characteristics including their high surface area-to-volume ratio, their ability to accumulate contaminants, and their ability to degrade or transform contaminants via numerous biochemical pathways (Mahlangu et al. 2024). Furthermore, because of the potential of the biomass from microalgae to provide additional benefits by yielding lipids, carbohydrates, and protein for use as feedstocks for biofuels, animal feed, or other biotechnological applications, the combination of using microalgae for bioremediation is an example of the integration of bioremediation within a circular bioeconomy (Mahmod et al. 2024).

C. sorokiniana and *T. wisconsinensis* are two of the microalgae that have been extensively studied because of their rapid growth rates, range of adaptability, in addition to prior biotechnological applications. Both of these belong to the Chlorophyta phylum. However, they markedly differ in their morphological, physiological, and biochemical characteristics. *C. sorokiniana* usually has a unicellular and spheroidal structure. It contains simple cellular architecture with a high division rate. In contrast, *T. wisconsinensis* forms coenobial colonies with somewhat thicker and more rigid cell walls that are structurally more complex and morphologically differentiated. Such inherent differences are expected to influence their responses to metal-induced stress. Arsenic exposure, in particular, may affect each genus through distinct uptake pathways, detoxification mechanisms, and tolerance strategies. A comparative evaluation of these two taxa therefore provides an opportunity to elucidate how algal morphology and physiology regulate arsenic interaction and removal.

Although algal bioremediation has received increasing attention, little work has been done on comparative studies. Very few studies have been conducted on the stress response of arsenite As(III) and arsenate As(V) together in various genera of green microalgae. Most of the work done has been on either As(III) or As(V) alone, and that too on a particular strain of algae. Hence, inter-specific variations and their impacts on bioremediation effectiveness and biochemical yield have not been given much importance. Thus, the comprehension of bioremediative stress response of morphologically diverse green microalgae due to arsenic is not comprehensive, especially when combined with metal detoxification and bioresource production.

The present study addresses this knowledge gap through a comprehensive comparative assessment of *C. sorokiniana* and *T. wisconsinensis* under As(III) and As(V) stress. The investigation encompasses morphological and molecular identification, growth kinetics, biomass production, pigment dynamics, ultrastructural alterations by scanning electron microscopy, and biochemical composition carbohydrate, protein, and lipid analyses. Quantification of arsenic removal efficiency was performed with ICP-MS. We hypothesize that differences in cellular architecture and metabolic regulation between *C. sorokiniana* and *T. wisconsinensis* govern their adaptive tolerance and arsenic removal capacity. These traits may be exploited for sustainable wastewater treatment and biofuel production. We further propose that the two genera employ distinct biochemical pathways and structural mechanisms for arsenic detoxification. Such divergence may enable their concurrent and complementary application in integrated biotechnological systems. The findings of this study are expected to advance understanding of species-specific arsenic interactions in green microalgae. They will also support the development of bioprocessing strategies that couple bioremediation with bioenergy production.

Materials and methods

Microalgal strain and chemicals

The freshwater microalgal strain employed here was identified morpho- molecularly as *C. sorokiniana* and *T. wisconsinensis*, a genus well known for its environmental tolerance and biotechnological potential. The cultures were grown axenically in BG11 medium, autoclaved at 121 °C for 20 min prior to inoculation. Working solutions of sodium arsenite [$NaAsO_2$, As(III)] and sodium arsenate [$Na_2HAsO_4 \cdot 7H_2O$, As(V)] were each prepared at 1 g L^{-1} in deionized water and filter-sterilized (0.22 μm). All analytical-grade chemicals were purchased from Merck (India) and the culture media employed for experiments were acquired from Hi-Media Laboratories (India).

Microalgae were grown in 250 mL flasks containing 160 mL BG11 at 25 ± 2 °C, 16:8 h light–dark cycle, and 108 μmol photons m^{-2} s^{-1} illumination. All experiments were performed in triplicate to ensure reproducibility.

Experimental outline

The study assessed the physiological, biochemical, ultrastructural, and bioremediation reactions of *C. sorokiniana*. and *T. wisconsinensis*to arsenite [As(III)] and arsenate [As(V)] stress. Cultures were subjected to six concentrations (0–125 mg L^{-1}) and monitored in triplicate for growth and pigment content over a 25-day trial at 5-day intervals. On day 25, total biomass was collected, washed, and dried for biochemical analysis of carbohydrates, proteins, and lipids, and the remaining medium was assessed for arsenic concentration to calculate reduction efficiency. Morphological and ultrastructural changes for the 125 mg L^{-1} and control conditions were investigated using a combination of phase contrast microscopy and scanning electron microscopy. This experimental design allowed for assessment of both dose and time dependent responses and the reciprocal relationships under conditions of arsenic stress, physiological acclimation, and remediation capacity. The combined approaches provided more advanced understanding of stress physiology and underlined the promise of *C. sorokiniana*. and *T. wisconsinensis* in terms of remediation and biofuels considerations.

Pure culture development

Collected algal samples were initially inoculated on BG11 agar plates and incubated in a controlled culture room under a light intensity of 108 μmol photons m^{-2} s^{-1}, a photoperiod of 16:8 h light–dark at 24 ± 2 °C for 48–96 h. Algal colonies that appeared were picked and restreaked onto fresh BG11 agar plates to encourage the growth of individual and well-separated colonies. After the formation of distinct colonies, they were analyzed microscopically to confirm morphological homogeneity and then inoculated into 50 mL of BG11 liquid medium. Pure isolates of each species were then scaled up in 250 mL of BG11 medium to create mother cultures for further experiments.

Morphological and molecular identification of microalgae

The microalgal strains were isolated from different water bodies and soil of Midnapore and Purulia (West Bengal), and analyzed under high-magnification microscope (Carl Zeiss, Primo Star, Germany) under 1000× magnification. The micrographs were taken by a digital camera attached to the microscope. Cells were observed for colony arrangement, shape, size, cell wall

characteristics, and presence of spines or other structural features. Taxonomic assignment of isolates was done with the help of the online algal database and Freshwater Algal Flora of the British Isles .

For molecular identification, genomic DNA was extracted using the CTAB method with slight modifications. The 18S rRNA gene region was amplified using universal primers in a thermal cycler (Bio-Rad). The PCR products were purified using a Qiagen PCR purification kit and sequenced commercially (Nalgen Bio, India). Sequence similarity was determined using BLAST (Basic Local Alignment Search Tool) against the NCBI GenBank database. This molecular confirmation strengthened the morphological identification and validated the strain identity for further experiments.

Determination of growth

The growth of *C. sorokiniana* and *T .wisconsinensis* was determined spectrophotometrically at 750 nm. 4 mL culture was taken at each time point, centrifuged at 5000 rpm, 10 min, 20 °C (Eppendorf 5424, USA), and the pellet suspended in 4 mL distilled water. After homogenization, OD at 750 nm (Havlik et al. 2022) was determined (HITACHI U-2910). Specific growth inhibition, as a percentage of the control, measured arsenic-induced suppression and indicated tolerance and physiological adjustment under stress.

Assessment of biomass production in microalgae

Biomass concentration was measured gravimetrically at day 0 and day 25 under arsenite and arsenate stress. For each sampling point, 20 mL cultures were centrifuged, washed, and dried to constant weight. Dry weight (g L^{-1}) was employed to determine growth performance, enabling comparison between control and treatments and revealing the physiological responses of *C. sorokiniana* and *T. wisconsinensis* under arsenic exposure could be done. Biomass productivity (Al-Mallahi et al. 2023) and the percentage increase in biomass per liter per day were quantified using following equations (Kumar et al. 2016):

$$\%\ \text{Increase in Biomass Yield } (mg^{-1}\ Day^{-1}) = \frac{\text{Final dry weight (mg)} - \text{Initial dry weight (mg)}}{\text{Initial dry weight (mg)} \times \text{Culture volume (ml)} \times \text{Total culture days}} * 100$$

Assessment of chlorophyll content

Chlorophyll a and b concentrations were measured according to Lichtenthaler (1987). 4 mL culture was centrifuged (5000 rpm, 10 min, 20 °C), and pellets were removed in 100% acetone (5 mL). Extracts were kept in the dark at 4 °C for 24 h, then re-centrifuged, and absorbance read in the supernatant at 663.2 nm and 646.8 nm. Chlorophyll a, b, and total chlorophyll concentration were then calculated by using the following equations.

Chl a: $C_a = 12.25\ A_{663.2} - 2.79\ A_{646.8}$ (μg mL^{-1})

Chl b: $Cb = 21.50\ A_{646.8} - 5.10\ A_{663.2}$ (μg mL^{-1})

Total Chl= Chl a + Chl b (μg mL^{-1})

Chlorophyll content, normalized to biomass, revealed photosynthetic efficiency and stress-related pigment degradation under arsenic stress.

Microscopic assessment of morphological alterations

Morphological alterations upon arsenic stress were evaluated through phase-contrast microscopy (Carl Zeiss Primo Star) at 1000× magnification. Control and 125 mg L^{-1} arsenic-treated samples (Day 28) were observed for a change in cell shape, colony integrity, and structural deformities. Photomicrographs exhibited distinct stress-induced alterations such as thickening of the cell wall, shrinkage, fragmentation of the colony, and abnormal elongation. Qualitative observations were proved through visual evidence of arsenic-induced stress supported by ultrastructural findings through SEM.

Ultrastructural analysis using SEM

For SEM (Zeiss Sigma 300 VP-FESEM) analysis, cell pellets of control and 125 mg L^{-1} arsenic treated samples (Day-28) were fixed in 2.5% glutaraldehyde (PBS, pH 7.4) at 4 °C for 4 h, washed, dehydrated in an ethanol gradient (30%, 50%, 70%, 90%, and 100%), critically point-dried, mounted on stubs, and gold-coated (Tang and Foo 2024). The prepared samples were mounted onto the SEM platform to investigate detailed surface morphological alterations

Quantification of biomolecules

Carbohydrate content was quantified via the phenol–sulfuric acid method (Ansari et al. 2017) with some modification, a popular colorimetric assay in algal research. Briefly, microalgal extracts were reacted with concentrated sulfuric acid and 5% phenol, and the resulting chromophore was measured at 490 nm. Calibration was done through a glucose standard curve.

Protein content was measured by the Lowry method (Ganguly et al. 2024).. Alkaline copper reagent and then Folin–Ciocalteu's phenol reagent were added to the cell extract, yielding a stable blue complex. The absorbance was measured at 750 nm and the protein concentration was calculated using a bovine serum albumin (BSA) standard.

Lipid content was analyzed by the sulfo-phospho-vanillin (SPV) test (Ganguly et al. 2024). Dried algal mass was hydrolyzed in concentrated sulfuric acid at 100 °C for 10 min, and then freshly prepared phospho-vanillin reagent (vanillin in ethanol, diluted with deionized water and added phosphoric acid) was added to it. Absorbance was measured after incubation at 530 nm using canola oil as a reference standard.

Arsenic [As(III)] and [As(V)] quantification

Arsenic concentrations in culture supernatants were analyzed by ICP-MS. Control and 125 mg L^{-1} arsenic treated samples (Day-28) were centrifuged, filtered supernatants (0.22 μm), and acidified with 2% HNO_3. Calibration used certified 1000 mg L^{-1} arsenic standards with a detection of 0.5 μg L^{-1}. The method allowed for sensitive and reproducible measurement of remaining arsenic, which provided reliable data to calculate removal efficiency and uptake kinetics (Ganguly et al. 2024).

$$\text{Removal efficiency (RE\%)} = \frac{C_0 - C_i}{C_0} * 100$$

where, C_0 and C_i are initial and final As concentrations (mg L^{-1}), respectively.

Statistical Analysis

All experiments were performed in triplicate. GraphPad Prism (version 8.4.2) software was utilized for performing all statistical analysis. Two-way ANOVA was applied to analyze growth and chlorophyll data. The biomass productivity as well as biochemical analyses (carbohydrate, lipid, protein) were analyzed using a one-way ANOVA. To assess arsenic removal efficiency was calculated using a paired t-test. All tests were conducted to determine if any differences in treatment groups were statistically significant at the $p \leq 0.05$ level.

Results and discussion

Morphological and molecular identification of the microalgae

Morphological traits alone are often insufficient for the accurate identification of microalgal species. This limitation arises from pronounced phenotypic plasticity and the strong influence of environmental conditions on cellular morphology (Shrivastav et al. 2015). Therefore, reliable taxonomic identification requires the combined use of morphological and molecular approaches (Suarez-Montes et al. 2021).

Two freshwater microalgal isolates, designated as SPEC 1 and SPEC 2, were collected from different locations in West Bengal, India. Isolate SPEC 1 was obtained from freshwater ponds at Kanikha (22.382513 N, 87.47564 E). Light microscopic observations showed elongated or spindle-shaped cells. These cells typically formed coenobia consisting of four cells arranged in linear or slightly curved rows. Individual cells measured approximately 6–12 μm in length and 2–4 μm in width. The cell walls were smooth, and the ends were pointed. Each cell contained a parietal chloroplast without a distinct pyrenoid. No mucilaginous sheath was observed. These characteristics are typical of the genus *Tetradesmus*. However, morphological similarities with closely related species, such as *Tetradesmus dimorphus* and *Tetradesmus obliquus*, made molecular confirmation necessary.

Isolate SPEC 2 was collected from a freshwater stream in the Barria (23.212595 N, 86.106403 E). The cells were unicellular and spherical to slightly oval in shape. They occurred predominantly as solitary individuals. Cell diameters ranged from 3 to 8 μm. The cells possessed

smooth and rigid cell walls. A single cup-shaped parietal chloroplast was present, along with a clearly visible pyrenoid surrounded by a starch sheath. Flagella and mucilaginous envelopes were absent. These features are characteristic of the genus *Chlorella*. However, species-level identification based solely on morphology remained uncertain.

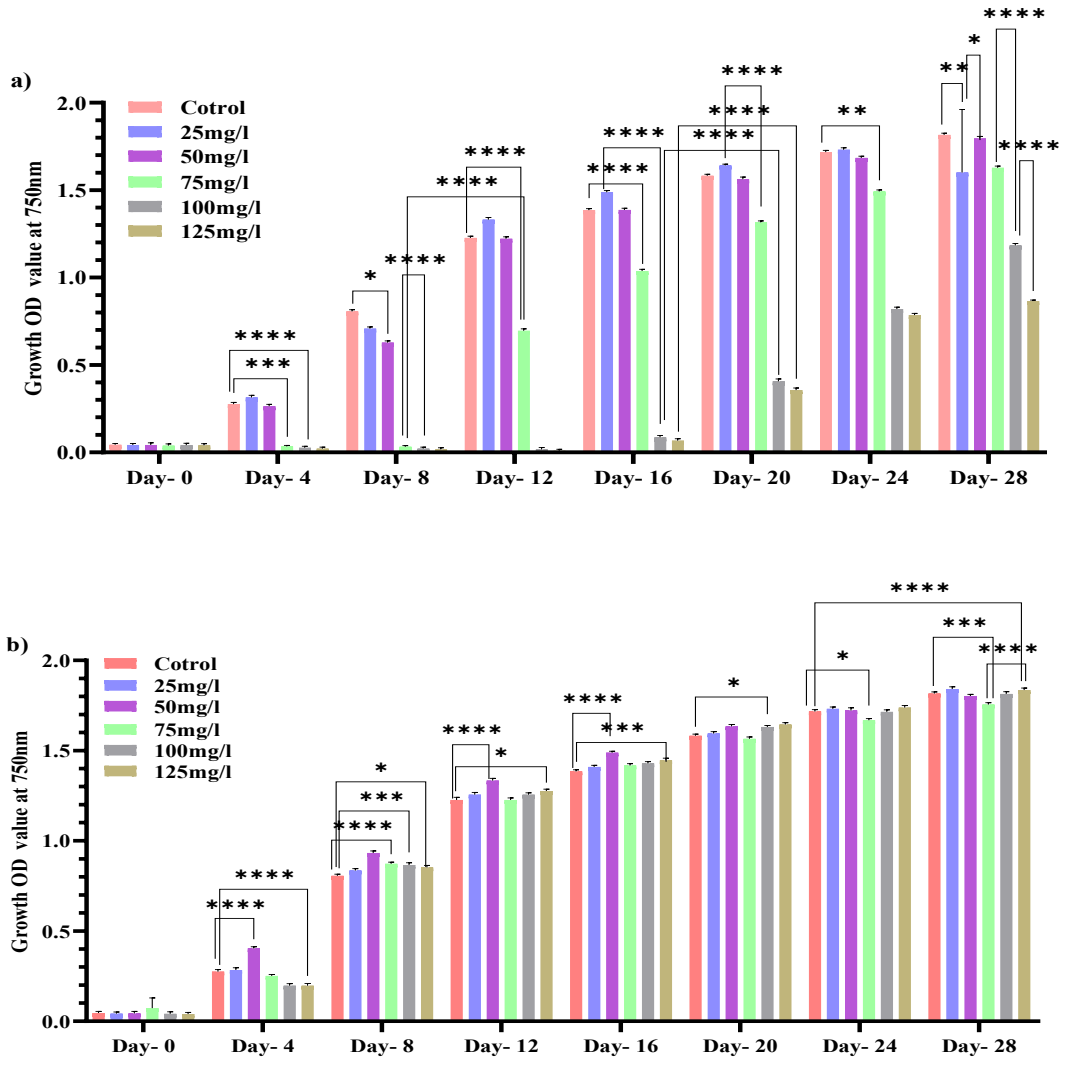
Molecular characterization of both isolates was carried out using the 18S rRNA gene, a widely accepted marker for microalgal DNA barcoding (Minhas et al. 2016). Genomic DNA was extracted from the algal biomass. The target gene was amplified using universal primers and subsequently sequenced. The obtained sequences were compared with reference sequences in the NCBI GenBank database using the BLASTn algorithm. The sequence of SPEC 1 showed 99.23% similarity with *Tetradesmus wisconsinensis* (AB037097.1). The sequence of SPEC 2 exhibited ≥99% similarity with reported *Chlorella* species. Based on the agreement between morphological and molecular data, SPEC 1 was identified as *Tetradesmus wisconsinensis* (GenBank accession: PX454383), while SPEC 2 was identified as *Chlorella sorokiniana* (GenBank accession: PX796505).

Growth parameter

Variation in the growth response of *C. sorokiniana* and *T. wisconsinensis* under different concentrations of [As(III)] and [As(V)]

C. sorokiniana and *T. wisconsinensis* exhibited different patterns of growth in response to arsenite [As(III)] and arsenate [As(V)] stress, indicating that each species utilises unique tolerance mechanisms and toxic effects (Fig. 2). In *C. sorokiniana* the response to arsenite was biphasic, the low concentrations of (25-50 mg L^{-1}) were either sustained or had a stimulatory effect on growth as a result of hormesis related to enhancing antioxidant defences and enhancing detoxification through Acr3-mediated excretion and GSH/phytochelatin complexation (Liu et al. 2010; Villadangos et al. 2011). Conversely, higher concentrations (75–125 mg L^{-1}) caused considerable early inhibition. Such early inhibition is attributed to high reactivity of arsenite with protein thiols, leading to disruption in PSII and carbon assimilation. However, partial recovery in the later stages indicated that tolerant subpopulations survived and gradually restored redox homeostasis (Shaghaleh et al. 2025) (Fig. 1a). Under arsenate stress, *C. sorokiniana* exhibited significant tolerance. Even low doses (25–50 mg L^{-1}) were able to stimulate biomass growth.

The higher doses (75–125 mg L^{-1}) only led to mild and reversible inhibition. This reaction aligns with the phosphate-analog characteristics of arsenate, its reduced cytotoxicity, and the activation of compensatory energy-regeneration pathways (Levy et al. 2005) (Fig. 1b).



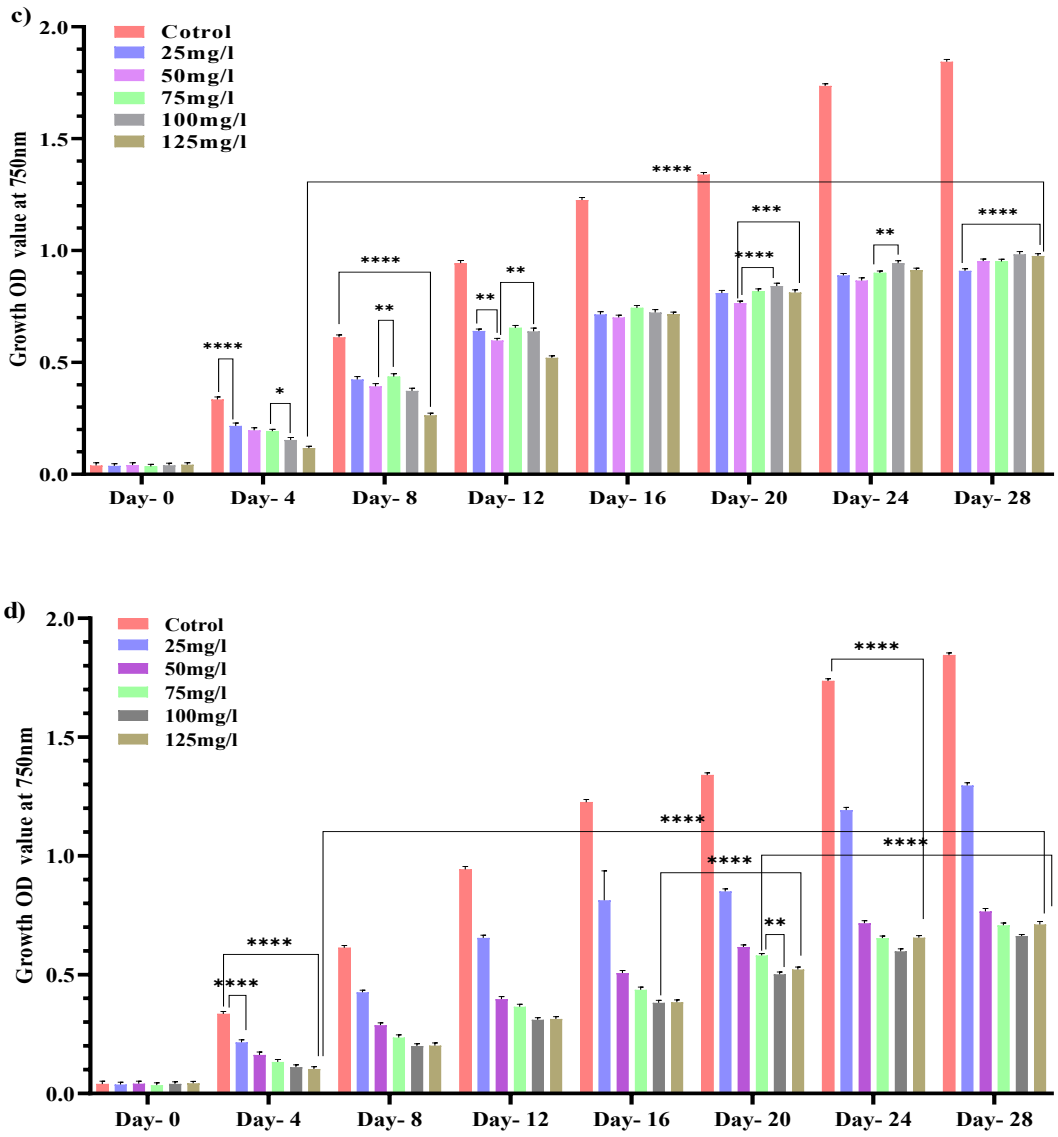
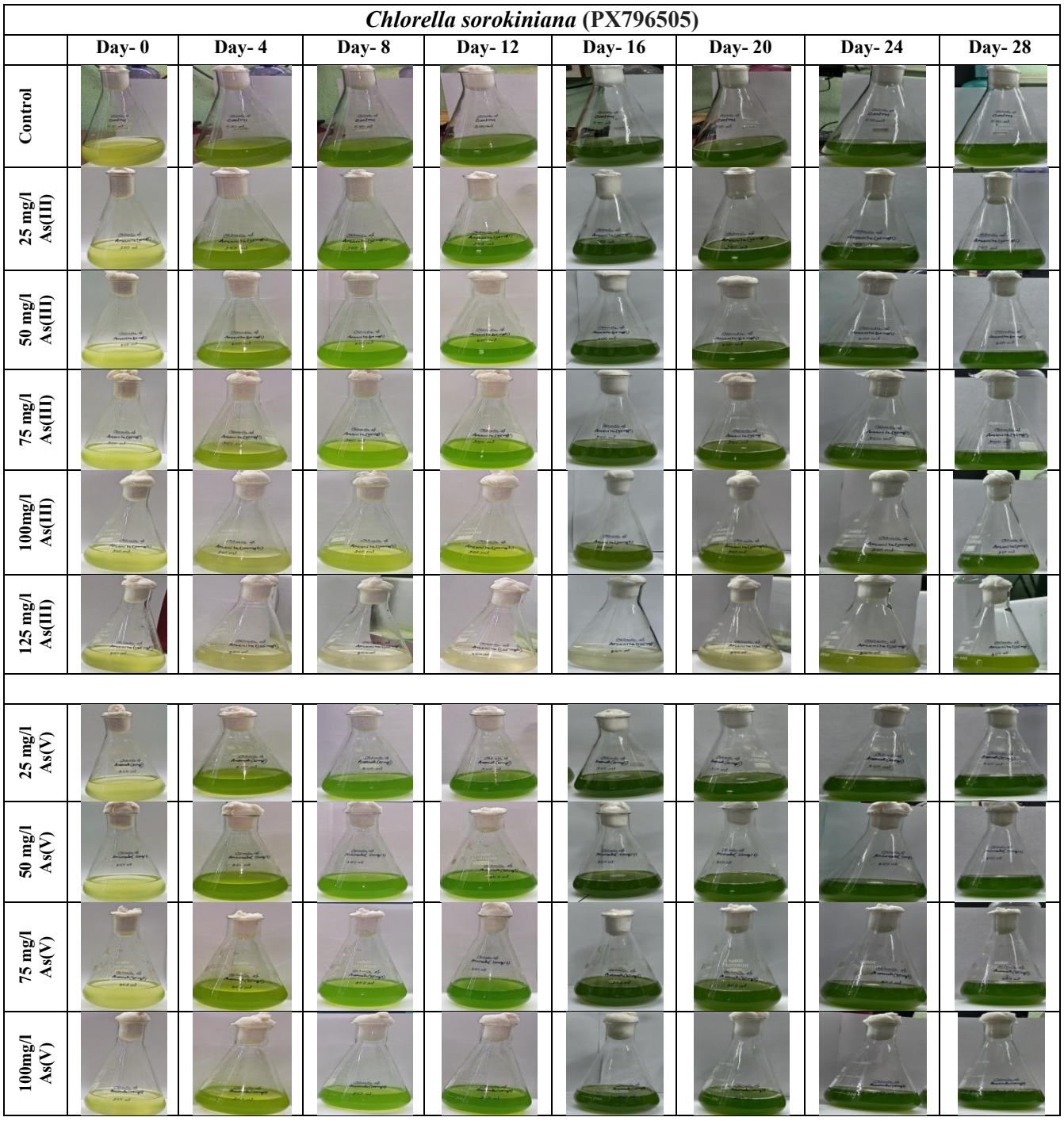


Fig. 1 Effects of varying concentrations of (a) As(III) and (b) As(V) on the growth of *C. sorokiniana*and (c) As(III) and (d) As(V) on the growth of *T. wisconsinensis*.The data are mean ± S D.obtained from triplicates (p**** < 0.0001, *p*** < 0.005, *p*** < 0.01, *p** < 0.05).

T. wisconsinensis exhibited more severe and sustained growth inhibition under both arsenic species. It faced strong early suppression in arsenite stress at 35–65%, which was due to impaired PSII electron transport, reduced chlorophyll synthesis, and ROS-driven metabolic damage. Later, partial recovery occurred that was supported by increased antioxidant enzyme activity and thiol-based detoxification (Kramárová et al. 2012) (Fig. 1c). Overall, arsenate induced even stronger toxicity in *T. wisconsinensis* than arsenite. Such inhibition was constant,

dose-dependent, and with a very slight late stage recovery. This was attributed to the competition of phosphate transport, disruption in ATP generation, and weak metabolic compensation (Rodríguez-Martín et al. 2022; Wang et al. 2013) (Fig. 1d). In contrast, *C. sorokiniana* showed greater tolerance to both As(III) and As(V), with particularly higher resistance to arsenate. *T. wisconsinensis*, however, remained highly sensitive to arsenate and recovered more slowly.



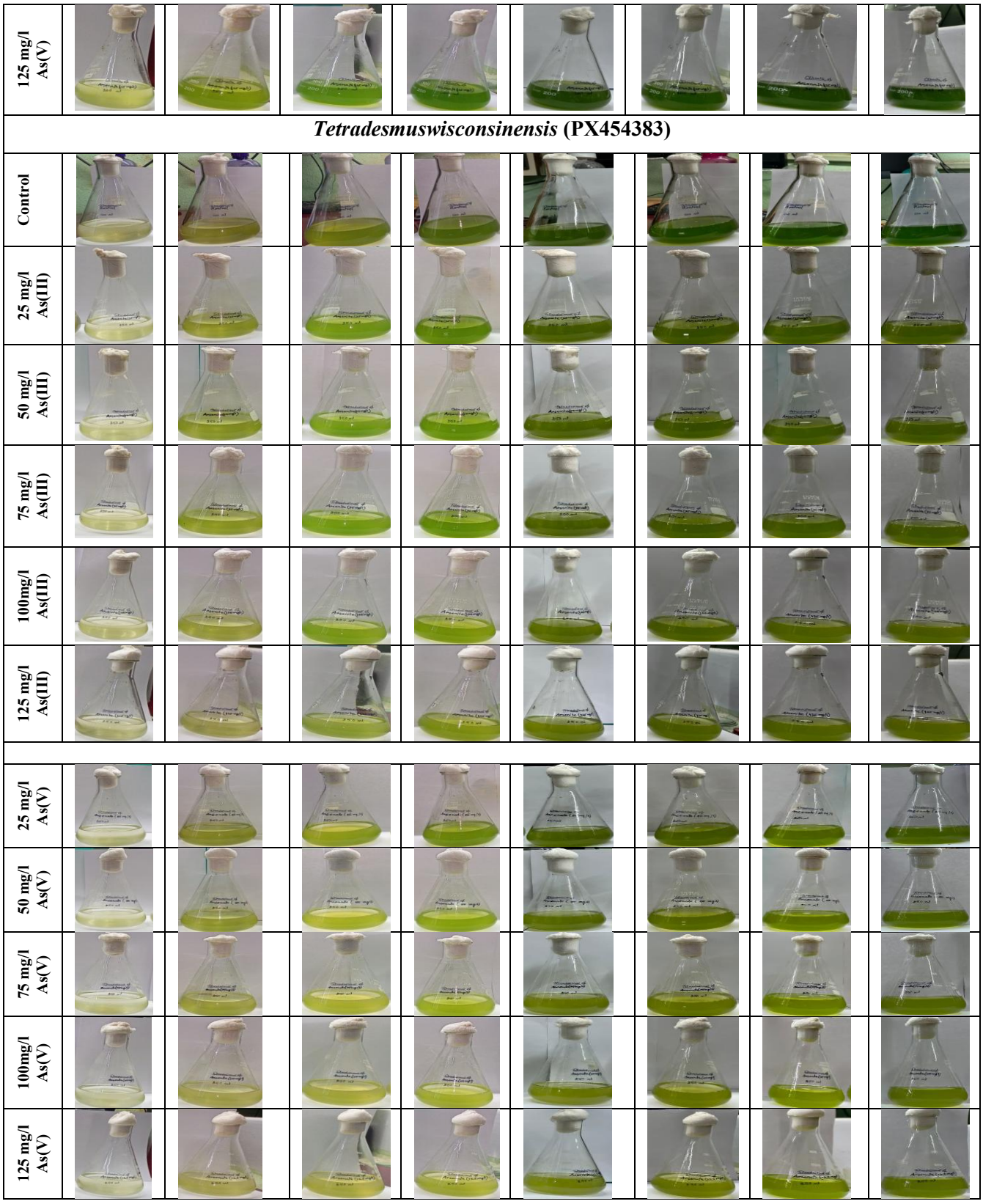


Fig. 2 A 28 days growth pattern of *C. sorokiniana* and *T. wisconsinensis* irradiated with varying As(III) and As(V) concentration

Biomass productivity

The percentage increase in biomass yield under arsenite [As(III)] and arsenate [As(V)] stress showed distinct species-specific tolerance patterns. *C. sorokiniana* exhibited a clear dose-dependent decline under As(III). Biomass decreased from 0.205 mg^{-1} day^{-1} in the control to 0.139 mg^{-1} day^{-1} at 125 mg L^{-1}. Such a decrease represents the high cytotoxicity of As(III), which is rapidly taken up by cells via aquaglyceroporins, disrupts protein thiols, generates ROS, and suppresses important photosynthetic and metabolic enzymes (Ali et al. 2009). A slight increase at 25 mg L^{-1} may be indicative of a hormetic effect where minor oxidative stress increases antioxidant activity and carbon assimilation for a short period (Piršelová et al. 2022) (Fig. 3a). In contrast, *C. sorokiniana* was highly tolerant of As(V). Its biomass remained stable over the range of 25–125 mg L^{-1}, between 0.209 and 0.212 mg^{-1} day^{-1}. This is because As(V) is a phosphate analog. While its entry is through phosphate transporters, the comparative toxicity is lower, and it may even trigger the phosphate-starvation response and ATP regeneration pathways, along with antioxidant defenses (Murray et al. 2003). These altogether support homeostasis in the cells under As(V) exposure (Fig. 3b).

T. wisconsinensis was more sensitive to arsenic stress in general. Biomass decreased by 55.2%, even at the low concentration of 25 mg L^{-1} As(III). A slight recovery at higher concentrations suggests the activation of detoxification pathways: glutathione–phytochelatin synthesis and osmoprotective metabolite accumulation. In the case of As(V), inhibition was even stronger and more sustained (a decrease of ~48–63% in biomass). Such strong phosphate-competition effects indicate the interruption of ATP generation, the synthesis of nucleic acids, and photophosphorylation (Wang et al. 2015) (Fig. 3c). In contrast, *C. sorokiniana* showed increasing tolerance under rising metal concentration and a higher metabolic flexibility. From these patterns, *T. wisconsinensis* displays greater vulnerability to both As(III) and As(V) toxicity; it is more sensitive, especially to As(V), due to differences in uptake mechanisms, redox regulation, and capacity for responses against stress (Fig. 3d).

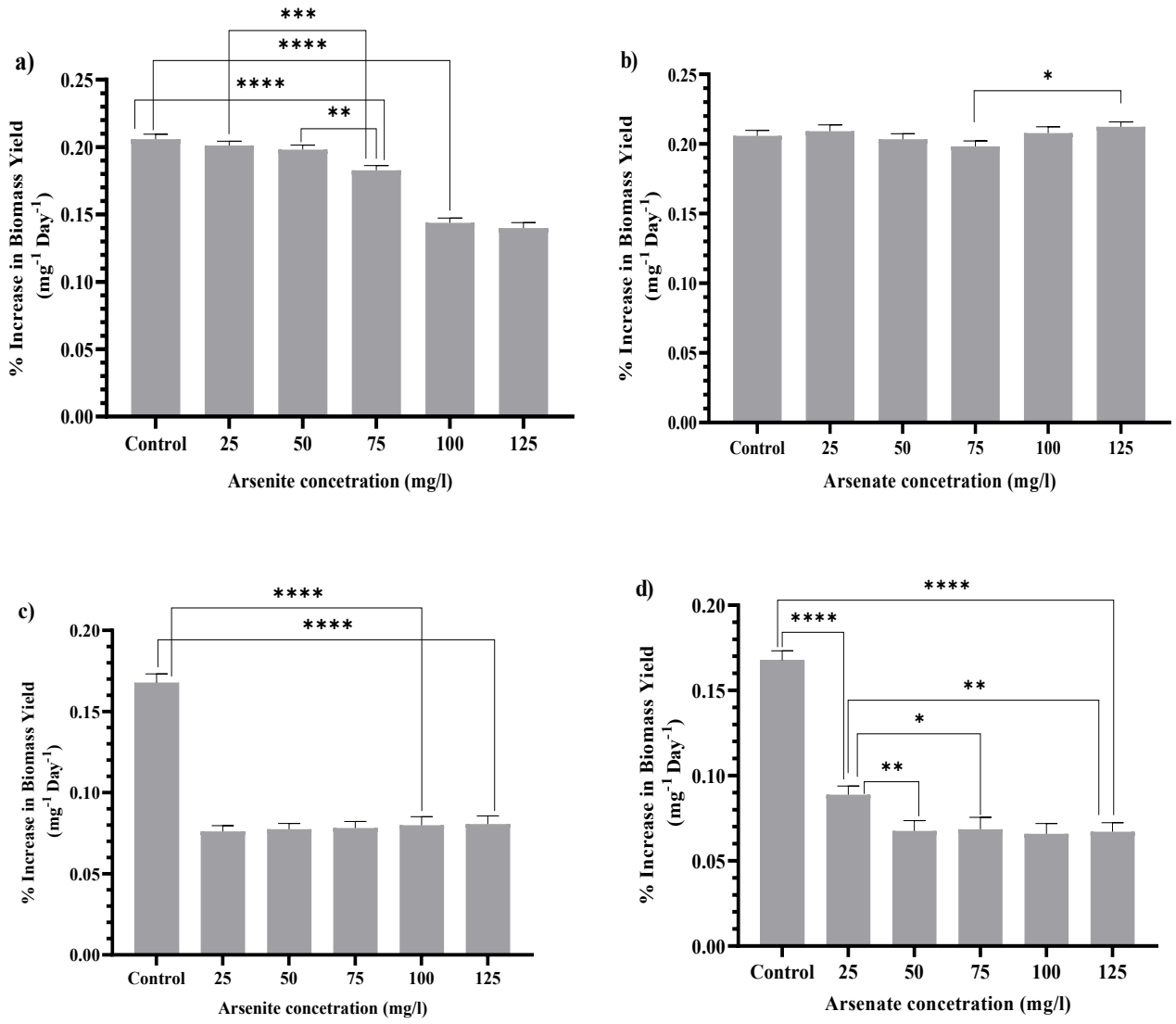


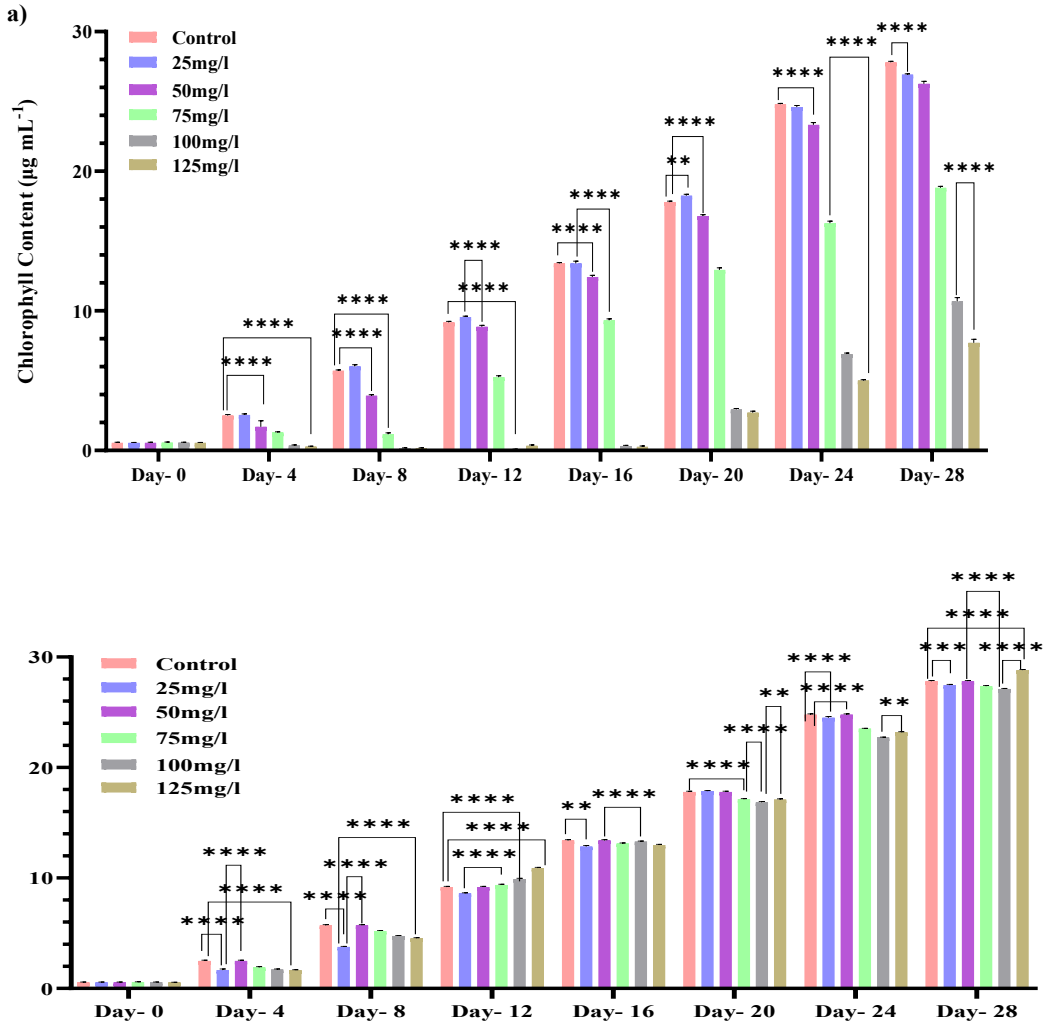
Fig. 3 Effects of varying concentrations of (a) As(III) and (b) As(V) on the biomass content of *C. sorokiniana* and (c) As(III) and (d) As(V) on the biomass content of *T. wisconsinensis*.The data are mean ± S D. obtained from triplicates (p**** < 0.0001, *p**** < 0.005, *p*** < 0.01, *p** < 0.05).

Modulation of chlorophyll content in *C. sorokiniana* and *T. wisconsinensis* under differential arsenic [As(III) and As(V)] stress

Total chlorophyll dynamics of *C. sorokiniana* and *T. wisconsinensis* under arsenite [As(III)] and arsenate [As(V)] stress showed marked species-specific sensitivity and acclimation patterns. Under As(III), *C. sorokiniana* suffered strong early chlorophyll inhibition in a clear dose-dependent manner. On day 4, the drop in chlorophyll ranged from 2.498 µg mL^{-1} in the control to 1.700–0.278 µg mL^{-1} at 50–125 mg L^{-1}. This reflects rapid uptake of As(III) through

aquaglyceroporins, ROS-driven breakdown of pigments, and direct inhibition of chlorophyll-synthesizing enzymes. At moderate stress (75 mg L^{-1}), *C. sorokiniana* showed a marked recovery. Chlorophyll increased from 1.155 µg mL^{-1} on day 8 to 18.811 µg mL^{-1} by day 28, reaching about 87% of the control. This rebound suggests activation of antioxidant defenses, thylakoid repair, and improved photosystem stability. Higher concentrations (100–125 mg L^{-1}) showed only partial recovery, with day-28 values of 10.677–7.704 µg mL^{-1}, suggesting persistence of oxidative stress (Patel et al. 2018) (Fig. 4a). In contrast, *T. wisconsinensis* had only moderate early inhibition, between 20–41%, and exhibited a more gradual acclimation response. Its chlorophyll levels reached only 11.55 to 11.92 µg mL^{-1} by the late stages, or approximately 53 to 55% of the control. This pattern indicates slower but sustained adaptation driven by antioxidant activity, vacuolar sequestration, and membrane remodeling (Greipel et al. 2024) (Fig. 4c).

Under As(V), the differences became more marked. *C. sorokiniana* exhibited, at moderate dosages, 50 mg L^{-1}, levels of chlorophyll close to that of the control. Only mild inhibition (<10%) showed up at 75–100 mg L^{-1}. At 125 mg L^{-1}, chlorophyll even showed slight stimulation (28.806 µg mL^{-1}; +3.6%), indicating a hormetic response driven by enhanced phosphate transport, ATP regeneration, and reductive metabolism (Jiang et al. 2011) (Fig. 4b). In contrast, *T. wisconsinensis* exhibited high and sustained chlorophyll suppression across As(V) treatments. Early inhibition ranged from 42 to 50%. In a time course pattern, this inhibition increased to 58–94% by day 12 and remained 23–75% lower than the control even on day 28. This long-term decline reflects disturbed phosphate-dependent ATP synthesis, lowered Calvin cycle activity, reduced chlorophyll biosynthesis, and oxidative damage to thylakoid membranes (Hofslagare et al. 1994) (Fig. 4d).


a)
Chlorophyll Content (µg mL-1)
Control
25mg/l
50mg/l
75mg/l
100mg/l
125mg/l
Day- 0
Day- 4
Day- 8
Day- 12
Day- 16
Day- 20
Day- 24
Day- 28
b)
Chlorophyll Content (µg mL-1)
Control
25mg/l
50mg/l
75mg/l
100mg/l
125mg/l
Day- 0
Day- 4
Day- 8
Day- 12
Day- 16
Day- 20
Day- 24
Day- 28

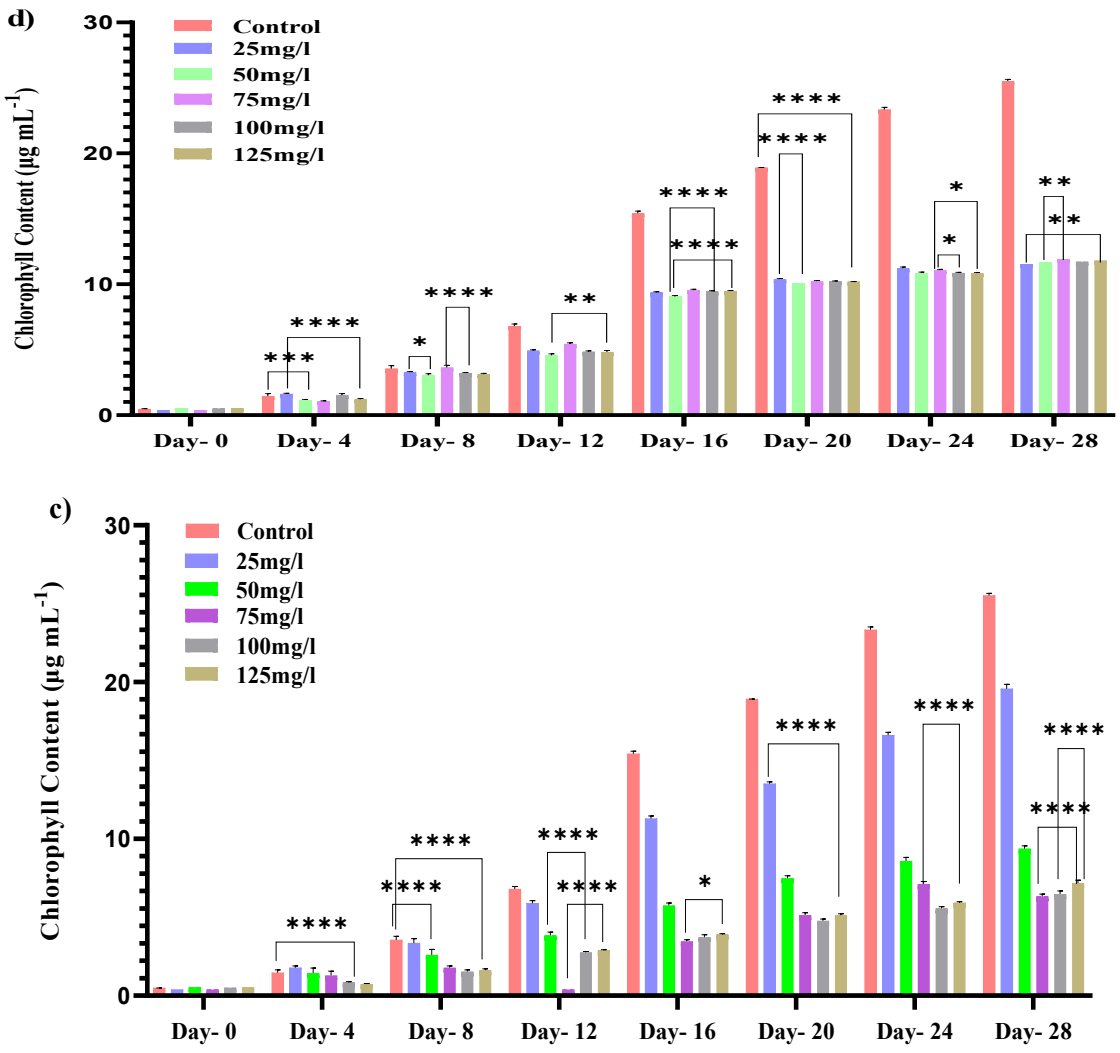


Fig. 4 Effects of varying concentrations of (a) As(III) and (b) As(V) on the chlorophyll content of *C. sorokiniana* and (c) As(III) and (d) As(V) on the chlorophyll content of *T. wisconsinensis*.The data are mean ± S D. obtained from triplicates (p**** < 0.0001, *p*** < 0.005, *p*** < 0.01, *p** < 0.05).

Morphological and ultrastructural alteration of *C. sorokiniana* and *T. wisconsinensis* under arsenic [As(III)] and [As(V)] stress

Microscopic and ultrastructural studies revealed species-specific responses to arsenic treatment in *C. sorokiniana* and *T. wisconsinensis* at a concentration of 125 mg/L. The control cells of *C. sorokiniana* possessed a normal structure. The shape was spherical to ellipsoidal. The surface was smooth, and the cell wall was intact. The cytoplasmic contents were evenly distributed both in compound and SEM. Arsenite [As(III)] resulted in extensive structural damage to *C.*

sorokiniana. The cells underwent contraction and margination. Pigmentation decreased substantially, and the cellular integrity was disrupted. Under SEM, there was extreme deformation, rupture, wrinkling, and pitting. Cell bursting occurred frequently, revealing a loss of turgor pressure and membrane integrity. Arsenate [As(V)] was less toxic. The cells underwent moderate deformation and reduction in size. The cells became rougher, while their structure remained intact (Díaz et al. 2020). The higher toxic potential of As(III) in *C. sorokiniana* can be associated with its affinity for protein thiol groups. It inhibits enzymes, alters redox states, increases ROS levels, and causes lipid peroxidation, ultimately causing membrane and wall disruption (Abbas et al. 2018) (Fig. 5).

Under control conditions, *T. wisconsinensis*had an organized coenobial arrangement. The cells had smooth and unbroken walls with distinct borders. Arsenic treatment brought about marked changes. Arsenite treatment led to slight morphological deformation, shrinkage, and unordered chloroplast localization. These indicate moderate oxidative damage. Arsenate treatment, however, led to severe harm. There was cell wall damage, membrane breakdown, and damage to the coenobium. This could be attributed to the higher affinity of cells to phosphate, thereby hindering ATP and chlorophyll biosynthesis, as well as oxidative damage by ROS (Nahar et al. 2022) (Fig. 5).

Overall, *C.sorokiniana* was more sensitive to arsenite, whereas *T. wisconsinensis* showed higher sensitivity to arsenate, reflecting differences in arsenic uptake and detoxification mechanisms.

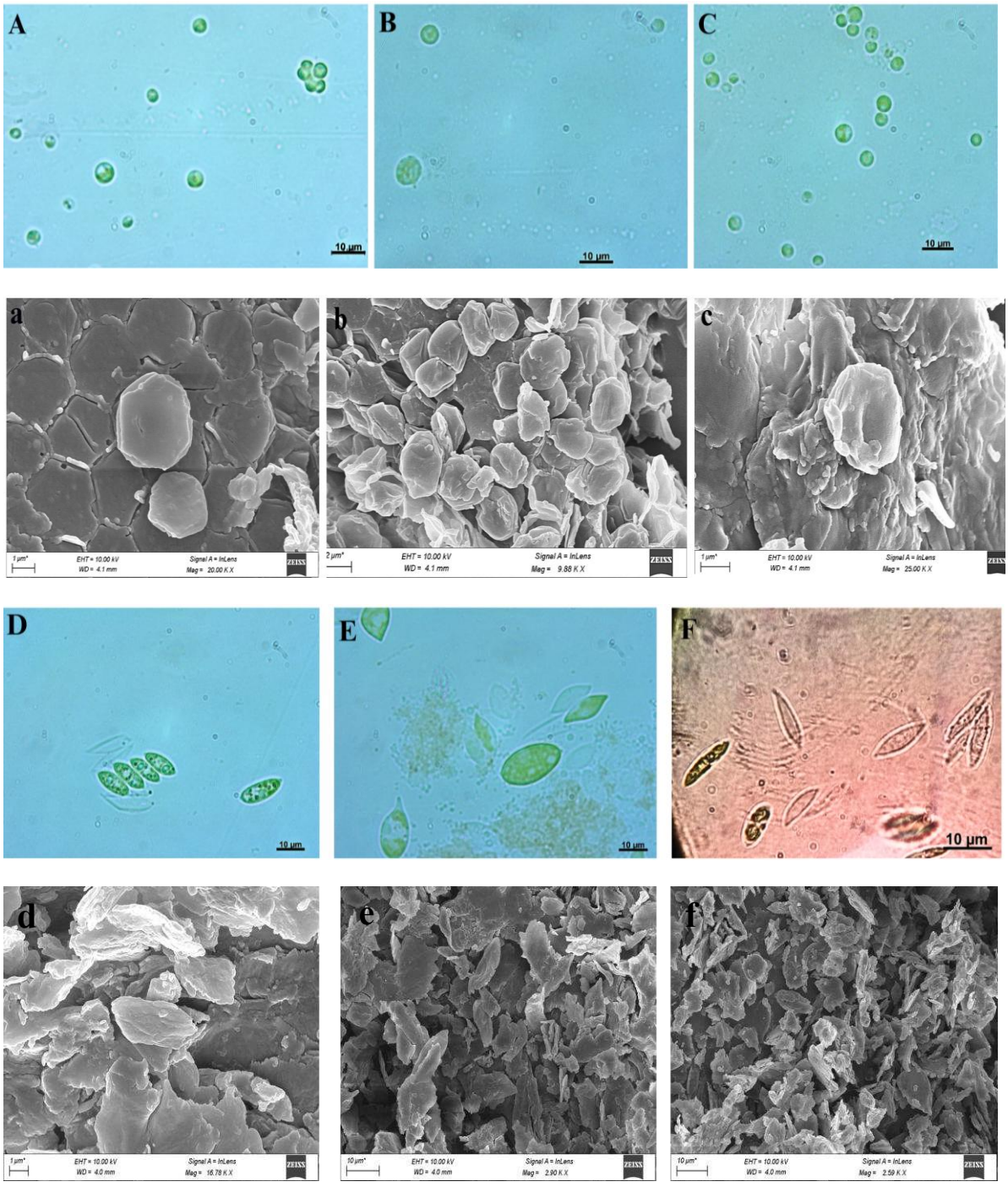
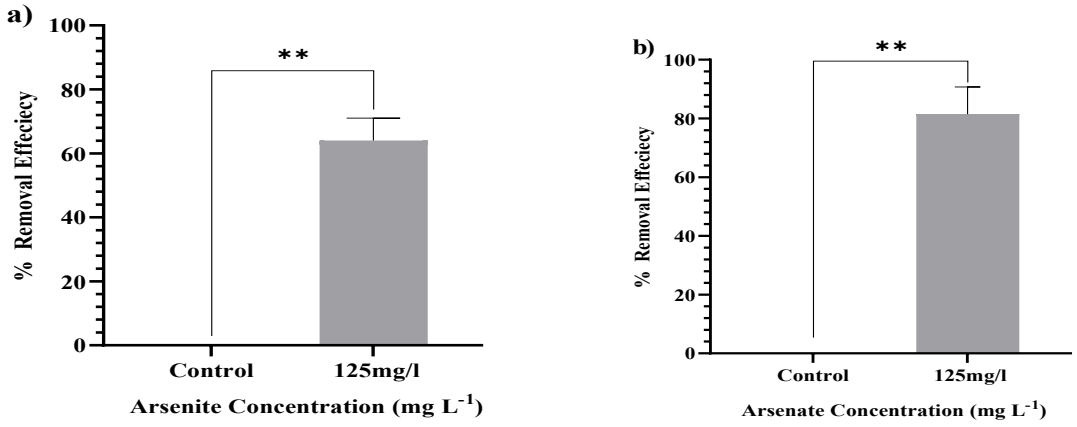


Fig. 5 Morphological alteration of *C. sorokiniana* through light microscope (A, B, C) image of control, 125 mg/l Arsenite and 125 mg/l Arsenate stress and Ultrastructural alteration of *C. sorokiniana* through SEM (a, b, c) image of control, 125 mg/l Arsenite and 125 mg/l Arsenate stress respectively and Morphological alteration of *T. wisconsinensis* through light microscope (D, E, F) image of control, 125 mg/l Arsenite and 125 mg/l Arsenate stress and Ultrastructural alteration of *T. wisconsinensis* through SEM (d, e, f) image of control, 125 mg/l Arsenite and 125 mg/l Arsenate stress respectively

Removal performance of trivalent [As(III)] and pentavalent [As(V)] arsenic species

C. sorokiniana and *T. wisconsinensis* exhibited a commendable arsenic remediation potential in 125 mg L^{-1} stress after 28 days. However, apparent species-specific differences occurred. The percentage of As(III) and As(V) removal by *C. sorokiniana* was 63.998% and 81.452%, respectively (Fig. 6a,b), whereas *T. wisconsinensis* showed even higher efficiency, removing up to 55.26% As(III) and 90.76% As(V) (Fig. 6c, d). Both algae removed As(V) more effectively because of its structural similarity with phosphate, allowing its uptake through high-affinity phosphate transporters; this allows fast intracellular accumulation. Inside the cell, it is reduced to As(III) by arsenate reductase and subsequently bound to glutathione or phytochelatins for safe vacuolar sequestration (Zhang et al. 2022). These steps enhance overall removal considerably. Moreover, As(V) exists as an anion ($H_2AsO_4^-$, $HAsO_4^{2-}$), which enables strong binding to positively charged sites of extracellular polymeric substances, enhancing biosorption (D'Abzac et al. 2012). In contrast, neutral As(III) (H_3AsO_3) exhibits poor surface binding and mostly enters cells via passive diffusion through aquaglyceroporins (Liu et al. 2002). As(III) has greater inherent toxicity due to its strong interaction with protein sulfhydryl groups and key metabolic enzymes, the result of which is that photosynthesis, growth, and biomass formation are inhibited, which in turn limits removal (Abbas et al. 2018). As(V) exerts relatively less stress and thus allows cells to sustain ATP production, antioxidant activity, and metabolic stability required for continued uptake and detoxification (Finnegan and Chen 2012). Among the two species, *T. wisconsinensis* proved to be the most efficient As(V) remover, giving a maximum overall removal efficiency of 90.76%. This superior performance is likely due to stronger surface adsorption and higher intracellular sequestration capacity.



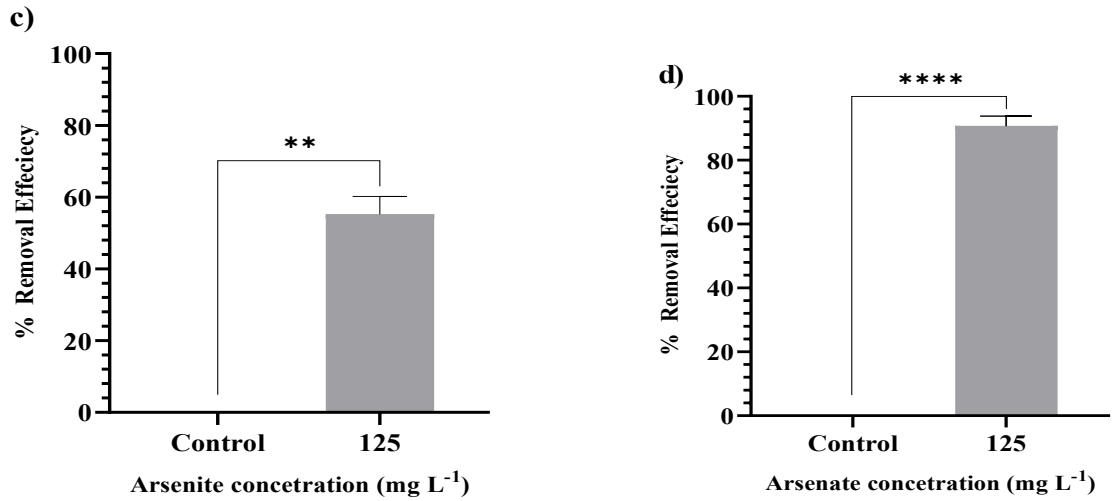


Fig. 6 Variation of metal removal percentage by *C. sorokiniana* with 125 mg/l concentration of (**a**) As(III), (b) As(V) and *T. wisconsinensis*of (c) As(III) and (d) As(V). The data are mean ± S D.obtained from triplicates (p**** < 0.0001, *p*** < 0.01).

Biochemical assessment

Modulation of carbohydrate content in *C. sorokiniana* and *T. wisconsinensis* under differential arsenic [As(III) and As(V)] stress

Both *C. sorokiniana* and *T. wisconsinensis* had dose-dependent bi-phase responses on carbohydrate content under 28-day arsenite As(III) and arsenate As(V) stress. However, there were more marks of recovery and overaccumulation in *C. sorokiniana*.

At *C. sorokiniana* with As(III) (Fig. 7a), there was a large decrease from 341.47 mg g^{-1} control values to 276.264 mg g^{-1} (-19.09%) at 25 mg L^{-1} and then 270.139 mg g^{-1} (-20.91%) at 50 mg L^{-1}. A subsequent increase began at 75-100 mg L^{-1} with 335.759 mg g^{-1} (-1.67%) and 328.65 mg g^{-1} (-3.75%). At 125 mg L^{-1}, there also was an increase to 350.901 mg g^{-1} (+2.76%), reflecting a very strong compensatory and osmoprotectant synthesis. At As(V) (Fig. 7b), there was an even stronger initial inhibition. Values fell to 309.269 mg g^{-1} (-9.41%), 253.923 mg/g (-25.64%), and 284.075 mg g^{-1} (-16.79%) at 25-75 mg L^{-1} (Alharbi et al. 2023). These reactions are ascribed to As(V) competition with orthophosphate and ATP disruption. A return began at 100 mg L^{-1} at 302.836 mg g^{-1} (-11.33%) and an over accumulation at 125 mg L^{-1} at 361.495 mg g^{-1} (+5.87%) with strong reprogramming (Choudhary et al. 2024). At *T. wisconsinensis*, there also was a weaker compensatory reaction. At As(III) (Fig. 7c), there had been an insignificant change from

control values at 341 mg g^{-1}. Values varied from 329.15 mg g^{-1} (-3.47%) and then 351.26 mg g^{-1} (+3.02%) at 25-100 mg L^{-1}. Values then fell at 308.00 mg g^{-1} (-9.68%) and 305.00 mg g^{-1} (-10.56%) and partially recovered at 336.61 mg g^{-1} (-1.29%). This reaction shows brief stimulation, subsequent photosynthesis inhibition, and insufficient acclimation. At As(V) (Fig. 7d), at *T. wisconsinensis*, there still was a constant reduction from 336.2 mg g^{-1}. Values then fluctuated at 310.54-322.16 mg/g (-4%-8%) at all concentrations with sparse recovery at higher doses. It shows low tolerance against phosphate analogy (Kofroňová et al. 2020).

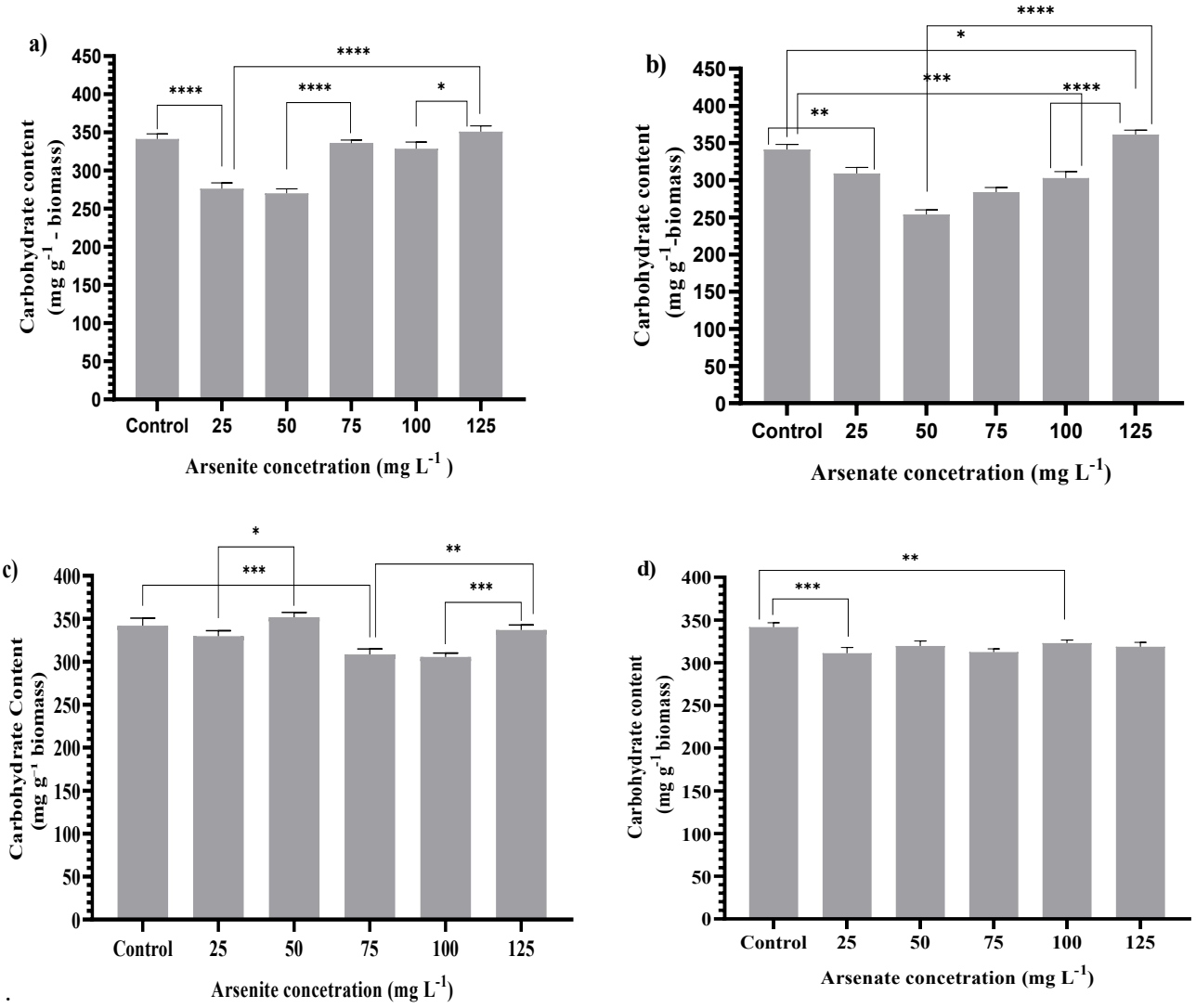
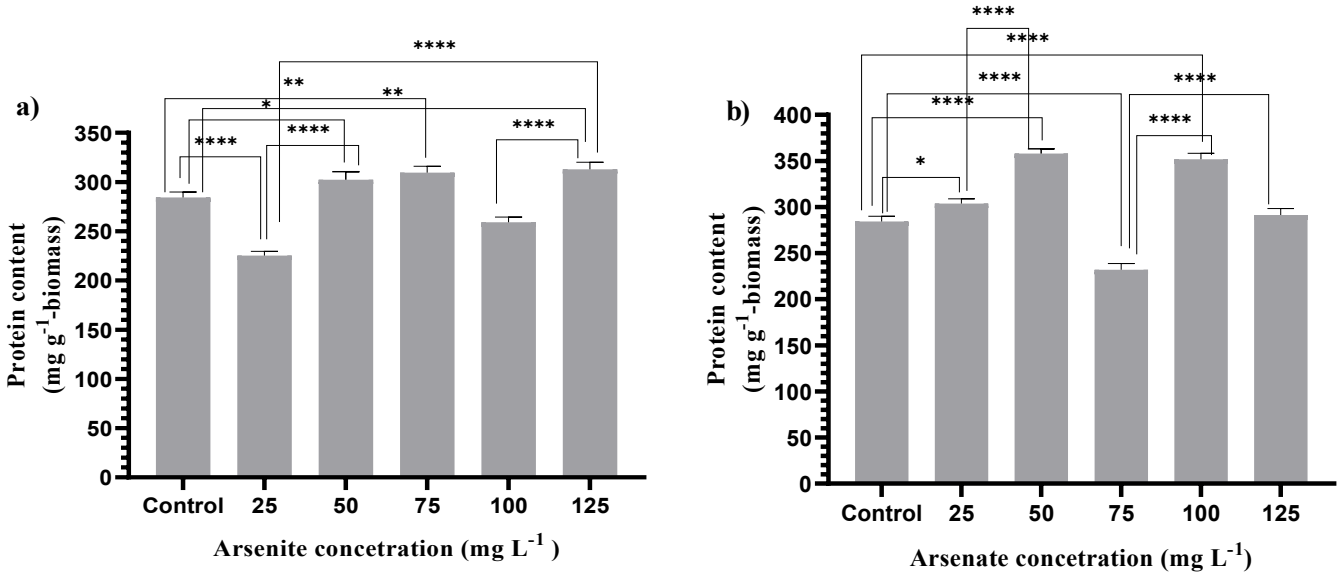


Fig. 7 Variation in carbohydrate content of *C. sorokiniana* with varying concentration of (**a**) As(III), (**b**) As(V) and *T. wisconsinensis*of (c) As(III) and (d) As(V).The data are mean± S D.obtained from triplicates (p**** < 0.0001, *p**** < 0.005, *p*** < 0.01, *p** < 0.05).

Modulation of protein content in *C. sorokiniana* and *T. wisconsinensis* under differential arsenic [As(III) and As(V)] stress

C. sorokiniana and *T. wisconsinensis* demonstrated specific and distinctive protein changes due to 28-day arsenite [As(III)] and arsenate [As(V)] stress. Both have adapted differently due to biochemical changes. *C. sorokiniana* demonstrated a reduction in total protein due to As(III) stress (Fig. 8a), that is, from 284.27 mg g^{-1} (control) at 25 mg L^{-1} to 225.31 mg g^{-1}. It implies stress-provoked degradation due to As(III) binding with sulfhydryl groups of enzymes. But at 50-125 mg L^{-1} concentrations, there was an increase in total protein at 302.32-312.99 mg g^{-1}. It implies synthesis of stress-provoked and antioxidant, heat-shock, and thiol peptide family proteins like glutathione and phytochelatins (Nowicka and Nowicka 2022). As(V) (Fig. 8b), *C. sorokiniana* evidenced an accumulated amount of protein. It reached its maximum at 357.94 mg g^{-1} at 50 mg L^{-1}. It might be due to phosphate-like uptake that aided ATP biosynthesis. At higher concentrations, protein oscillations are moderate (Xu et al. 2023). In contrast, *T. wisconsinensis* there were significant decreases in protein expression due to As(III) (-2.2% to -38.3%) (Fig. 8c) and As(V) (-15.7% to -23.4%) (Fig.8d). These cultures were more stress-sensitive due to arsenite. As(III) primarily affects cysteine residues. As(V) showed low stress response-mediated protein expression. Higher doses were beyond biosynthetic capabilities, and there were decreases at higher concentrations. It suggested a stress response activation for removal at biologically active doses (Tsuchiya et al. 2019).



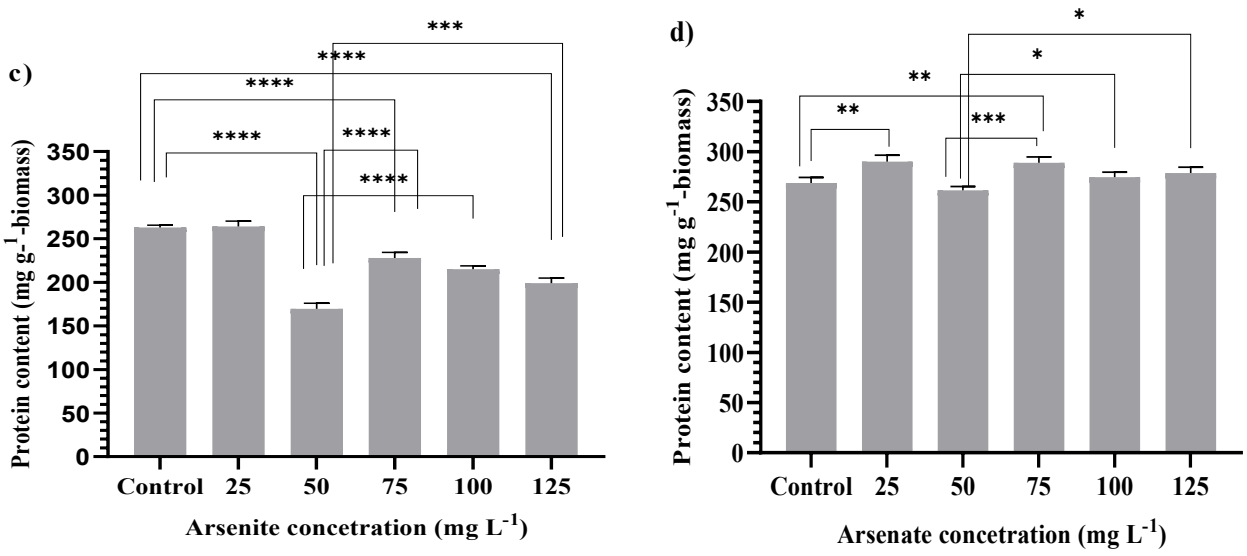


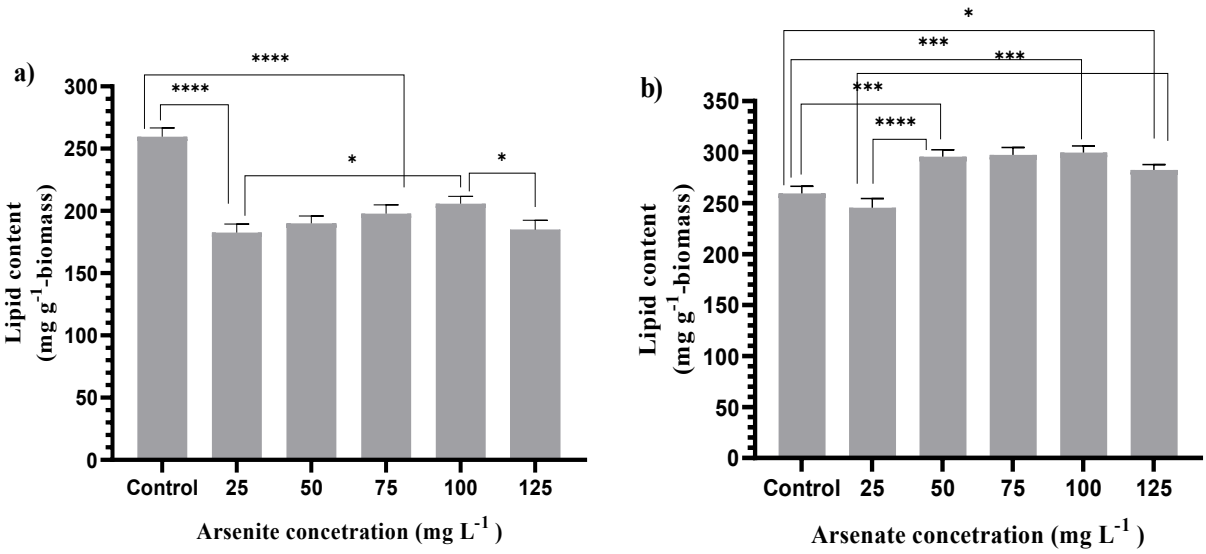
Fig. 8 Variation in protein content of *C. sorokiniana* with varying concentration of (**a**) As(III), (**b**) As(V) and *T. wisconsinensis* of (c) As(III) and (d) As(V).The data are mean ± S D.obtained from triplicates (p**** < 0.0001, *p**** < 0.005, *p*** < 0.01, *p** < 0.05).

Modulation of lipid content in *C. sorokiniana*and *T. wisconsinensis* under differential arsenic [As(III) and As(V)] stress

Arsenite [As(III)] and arsenate [As(V)] stress responses of *C. sorokiniana* and *T. wisconsinensis* were very different with regards to lipid accumulation. This variability occurred ranging from 0-125 mg/L for a period of 28 days. There are various differences based on species and arsenic species.

As(III) doses significantly reduced lipid levels in *C. sorokiniana* lipid accumulation were reduced from 259.581 mg g^{-1} in control cells to 182.696 mg g^{-1} at 25 mg L^{-1} (-29.62%). However, there was a limited return at medium doses, with lipid concentrations varying from 190.071-205.705 mg g^{-1} at 50-100 mg L^{-1}. Again, there was a drop at 125 mg L^{-1} to 184.806 mg g^{-1}. This pattern shows an enduring inhibition of fatty acids synthesis because of highly reactive thiol groups, ROS production, decreased activity of acetyl-CoA carboxylase, and disrupted NADPH regeneration (Arora et al. 2018; L. Zhang et al. 2019) (Fig. 9a). As(V), on the other hand, caused a positive response in *C. sorokiniana* lipid concentrations rose from 245.429 mg g^{-1} at 25 mg L^{-1} to a maximum of 299.521 mg g^{-1} at 100 mg L^{-1} with a percentage increase of 15.3%. This pattern shows moderate toxicity leading to compensatory mechanisms involving an increase in NADPH synthesis, acetyl-CoA carboxylase activity, and utilization of carbon for

accumulating neutral lipids (Zhang et al. 2025) (Fig. 9b). The lipid response in *T. wisconsinensis* was more pronounced for both arsenic species. At As(III), the lipid accumulation increased from 180.48 mg g^{-1} (control) to 259.97 mg g^{-1} at 25 mg L^{-1} As(III) (+44.06%). Although there were varying responses at different concentrations, lipid accumulation remained considerably high (218.33-263.34 mg g^{-1}). This might be due to efficient stress-mediated carbon sequestration into TAGs, pronounced antioxidant properties, and efficient NADPH production (Osada et al. 2017; Devadasu and Subramanyam 2021) (Fig. 9c). Compared to *C.sorokiniana*, at As(V) (Fig. 9d), lipid accumulation in *T. wisconsinensis* was even more pronounced. The maximum accumulation reached 302.36 mg g^{-1} at 100 mg L^{-1} As(V) (+67.58%). It might be due to efficient phosphate mimicry, which affects ATP-dependent carbohydrate and protein biosynthesis, thereby diverting all available carbon into lipid synthesis (Upadhyay et al. 2016; Singh et al. 2023). Compared to *C.sorokiniana*, *T. wisconsinensis* clearly had a higher lipid induction rate at both As(III) and As(V). It clearly depicts better stress-protecting abilities and an efficient lipid stressful adaptative mechanism. Therefore, *T. wisconsinensis* could be an efficient alternative candidate for arsenic stress biotechnology and stress-mediated lipid production.



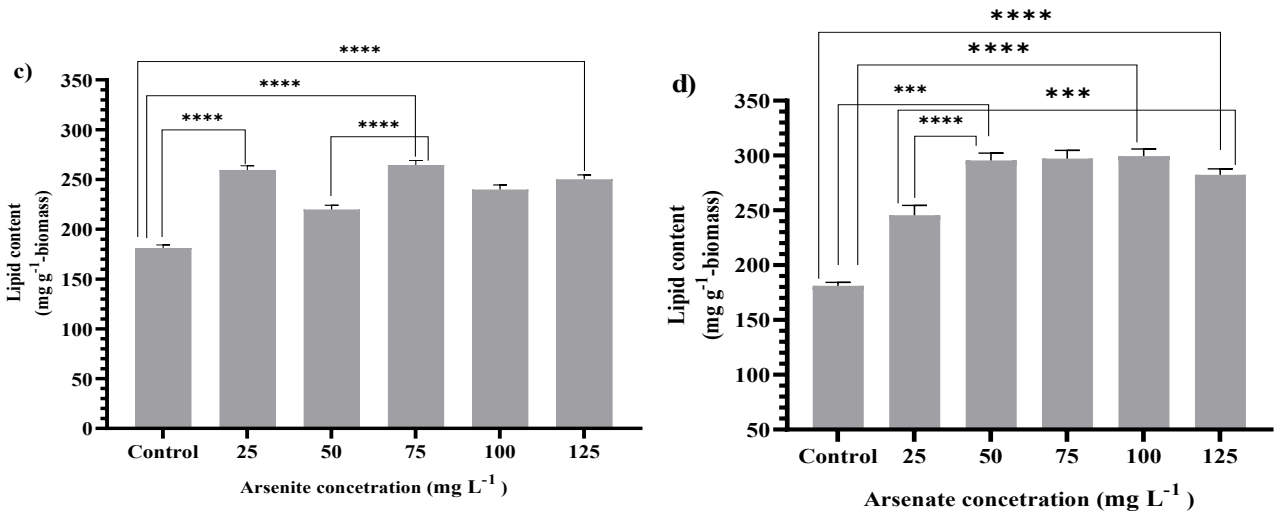


Fig. 9 Variation in lipid content of *C. sorokiniana*with varying concentration of (**a**) As(III), (**b**) As(V) and *T. wisconsinensis*of (c) As(III) and (d) As(V).The data are mean± S D.obtained from triplicates (p**** < 0.0001, *p**** < 0.005, *p** < 0.05).

Energetic trade-offs under arsenate stress

Arsenate exposure imposes a significant energetic burden on microalgal cells. It disrupts phosphate-dependent metabolism and increases the demand for detoxification and cellular maintenance. As a result, cells must rebalance carbon and energy allocation between growth, stress tolerance, and storage compound synthesis (Finnegan and Chen 2012). In *C. sorokiniana*, arsenate stress primarily supports physiological stability and sustained biomass production. Carbon flux is directed toward maintaining photosynthetic activity, protein synthesis, and cellular repair. This allocation supports stable growth and effective arsenic removal (León-Vaz et al. 2021). However, it limits the diversion of carbon toward lipid biosynthesis. Consequently, neutral lipid accumulation remains comparatively low under arsenate exposure. In contrast, *T. wisconsinensis* shows a distinctly different energetic response to arsenate exposure. Growth and photosynthetic investment are partially suppressed. At the same time, a larger fraction of fixed carbon is redirected toward lipid biosynthesis. This shift reflects stress-induced metabolic reprogramming that favors energy-dense storage compounds as a protective strategy (Alwaleed et al., 2025). Although this response reduces overall biomass productivity, it significantly enhances lipid accumulation. As a result, biomass quality for biofuel applications is improved.

Together, these contrasting responses demonstrate a clear energetic trade-off under arsenate stress. *C. sorokiniana* prioritizes growth stability and remediation performance, whereas *T. wisconsinensis* favors lipid enrichment at the expense of growth.

Mechanistic insights into arsenic uptake and intracellular detoxification

The differential responses of *C. sorokiniana* and *T. wisconsinensis* to arsenite [As(III)] and arsenate [As(V)] stress can be explained by known arsenic uptake and detoxification mechanisms in microalgae **(**Fig. 10). Arsenate is chemically similar to phosphate and is mainly taken up through phosphate transport systems. This direct competition interferes with cellular energy metabolism (Yang et al. 2012). In contrast, arsenite enters cells primarily through aquaglyceroporins because of its neutral and highly mobile nature. This pathway promotes rapid intracellular accumulation and results in higher toxicity (Muzaffar et al. 2022). The distinct inhibition patterns observed under As(III) and As(V) in this study are consistent with these speciation-dependent uptake mechanisms.

Cellular morphology plays an important role in regulating arsenic interactions at the algal surface. *C. sorokiniana* is unicellular and small in size, giving it a high surface-area-to-volume ratio. This feature likely enhances rapid arsenic adsorption and allows controlled uptake followed by efficient intracellular detoxification (Alharbi et al. 2023). In contrast, *T. wisconsinensis* forms coenobial colonies with thicker and more rigid cell walls. This structure may slow arsenic penetration but promote surface binding and prolonged exposure at the cell envelope. Such structural complexity likely contributes to delayed yet more pronounced stress responses, particularly under arsenate exposure (Shivaji and Dronamaraju 2019).

Once arsenic enters the cell, detoxification involves sequestration, transformation, and redistribution processes that are closely linked to carbon metabolism. In *C.sorokiniana*, sustained growth and relatively stable pigment levels under arsenate stress indicate effective metabolic adjustment. These responses suggest the maintenance of cellular homeostasis and efficient detoxification (Tang and Foo 2024). In contrast, *T. wisconsinensis* shows pronounced stress-induced lipid accumulation. This response reflects a shift in carbon partitioning toward neutral lipid synthesis as a protective strategy. Lipid-rich compartments may act as sinks for excess

reducing power or provide indirect protection against arsenic-induced oxidative stress (Alwaleed et al. 2025).

Overall, these findings indicate that arsenic tolerance in green microalgae is governed by both chemical speciation and morphology-driven uptake dynamics. Intracellular carbon allocation further modulates detoxification efficiency and stress adaptation. The contrasting behaviors of *C. sorokiniana* and *T. wisconsinensis* demonstrate how unicellular and coenobial architectures differentially influence surface adsorption, intracellular sequestration, and physiological resilience. These differences ultimately determine their suitability for bioremediation-focused or biofuel-oriented applications.

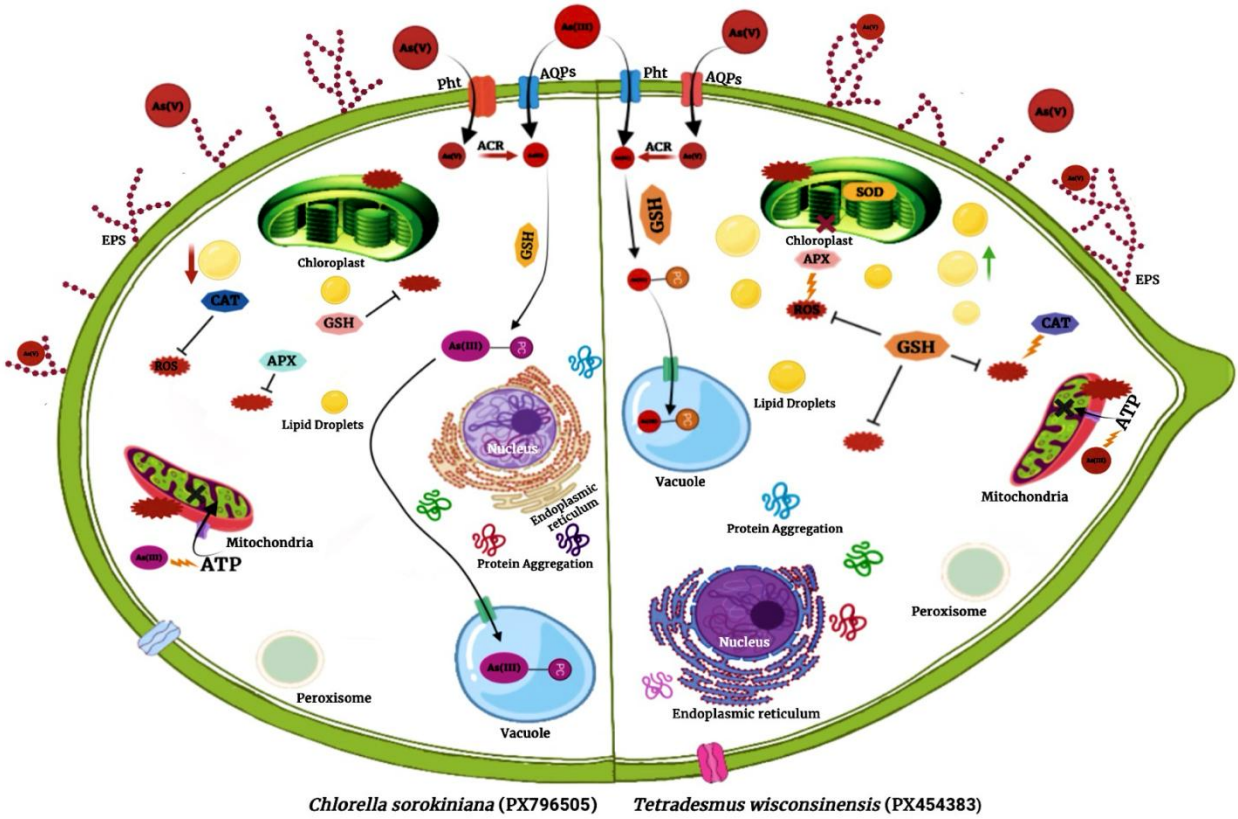


Fig. 10 Conceptual model illustrating arsenic tolerance mechanisms in *C. sorokiniana* and *T. wisconsinensis.*

Bioremediation efficiency and biofuel potential

The combined analysis of arsenic removal capabilities and biochemical changes indicates the practical feasibility of integrating microalgae-based bioremediation with biofuel-oriented

biomass utilization systems. Both *C. sorokiniana* and *T. wisconsinensis* effectively removed arsenite and arsenate. Simultaneously, they maintained the ability to accumulate energy-dense biomolecules even under arsenic stress. *C. sorokiniana* exhibited remarkable physiological stability in the presence of arsenate. Biomass production remained largely unchanged, and only limited alterations were observed in its biochemical composition. This characteristic suggests its suitability for long-term and continuous bioremediation systems. On the other hand, *T. wisconsinensis* showed stress-induced lipid accumulation under both arsenic forms. While growth was somewhat reduced, a metabolic reconfiguration towards neutral lipid synthesis was evident. Lipid enrichment was particularly pronounced in the case of arsenate, enhancing the fuel potential of the biomass.

These differing responses highlight the functional complementarity of the two species. Consequently, it is possible to design the process based on either purification efficiency or biomass quality. Overall, this approach proposes a sustainable integrated framework for pollution control and bioenergy production.

Environmental implementation

In the context of environmental applications, this research provides the scientific basis for using *C. sorokiniana* and *T. wisconsinensis* in low-cost and decentralized arsenic remediation systems. Such systems are particularly relevant for arsenic-affected regions in South and Southeast Asia. Both species demonstrated significant arsenic removal capabilities at environmentally acceptable concentrations. Their physiological stability was maintained even under prolonged arsenic exposure. These characteristics make them suitable for use in pond-based treatment systems and photobioreactor-based units. These systems are applicable to contaminated surface water, agricultural wastewater, and pre-treated groundwater.

The species-specific responses to different chemical forms of arsenic further enhance their practical potential. In oxygen-rich aquatic environments, arsenate [As(V)] is typically the predominant form. The high As(V) uptake capacity of *T. wisconsinensis* makes it suitable for phosphate-rich agricultural and municipal wastewaters, where the competition between phosphate and arsenate influences the removal process. On the other hand, *C. sorokiniana* maintained stable growth under both As(III) and As(V) stress. This tolerance ensures its

effectiveness in long-term systems with variable arsenic speciation. The integration of arsenic removal with biomass harvesting minimizes secondary waste production, addressing a significant limitation of conventional physicochemical methods. Instead of sludge production, this process generates valuable algal biomass, which can be further processed for biofuels or other value-added industrial applications. Overall, this research presents an integrated and sustainable framework that combines physiological responses, arsenic detoxification, and the economic utilization of biomass.

Conclusion

This study presents a comprehensive comparative analysis of *C. sorokiniana* and *T. wisconsinensis* under arsenite [As(III)] and arsenate [As(V)] stress. The results clearly demonstrate that the responses of the two species to arsenic stress are fundamentally different. Distinct species-specific variations were observed in physiological and biochemical parameters. Simultaneously, the chemical form of arsenic played a crucial role in determining the intensity and nature of these responses. Significant changes were observed in growth rate and chlorophyll content, indicating the impact of stress on photosynthetic processes. Alterations in macromolecular composition suggested metabolic adaptations. These findings demonstrate that arsenic speciation plays a central role in regulating stress tolerance and metabolic strategies in microalgae. *C. sorokiniana* maintained relatively stable growth and functionality even under prolonged arsenic exposure. The higher chlorophyll levels, particularly in the presence of arsenate, reflect its metabolic resilience and efficient adaptation. On the other hand, *T. wisconsinensis* accumulated significant amounts of lipids under both arsenic forms. This trend indicates stress-induced metabolic restructuring and a shift in carbon flux towards energy-dense compounds. Collectively, the results highlight the functional diversity between the two genera. *C. sorokiniana* primarily focuses on cellular stability and detoxification, while *T. wisconsinensis* is more active in producing bioenergy-related metabolites. Both species demonstrated effective arsenic removal capabilities at environmentally relevant concentrations without significant loss in biomass production. Notably, the high lipid accumulation in *T. wisconsinensis* strengthens its potential for biofuel feedstock production. Overall, this research provides a scientific basis for developing low-cost, sustainable, and environmentally friendly microalgal arsenic remediation

systems. At the same time, it opens up new horizons for the practical application of integrated bioremediation and bioenergy systems in arsenic-affected regions.

References

Abbas G, Murtaza B, Bibi I, Shahid M, Niazi N, Khan M, Amjad M, Hussain M, Natasha N (2018) Arsenic uptake, toxicity, detoxification, and speciation in plants: physiological, biochemical, and molecular aspects. International Journal of Environmental Research and Public Health 15(1):59

Alharbi RM, Sholkamy EN, Alsamhary KI, Abdel-Raouf N, Ibraheem IBM (2023) Optimization Study of the Capacity of *Chlorella vulgaris* as a Potential Bio-Remediator for the Bio-Adsorption of Arsenic (III) from Aquatic Environments. Toxics 11(5):439

Ali W, Isayenkov SV, Zhao F, Maathuis FJM (2009) Arsenite transport in plants. Cellular and Molecular Life Sciences 66(14):2329–2339

Al-Mallahi J, Ishii K, Sato M, Ochiai S (2023) Static supply of different simulated flue gases for native microalgae cultivation in diluted cow manure digestate. Journal of Environmental Management 335:117557

Alwaleed EA, Galal HRM, Aboueldahab M, Saber H (2025). Maximizing lipid accumulation in *Tetradesmus obliquus* under heavy metal stress for sustainable biodiesel innovation. BMC Biotechnology 25(1):20

Arora N, Dubey D, Sharma M, Patel A, Guleria A, Pruthi PA, Kumar D, Pruthi V, Poluri KM (2018) NMR-Based Metabolomic Approach To Elucidate the Differential Cellular Responses during Mitigation of Arsenic(III, V) in a Green Microalga. ACS Omega 3(9):11847–11856

Bashir L (2020) Arsenic poisoning: the risk, clinical features and treatment. Biomedical Journal of Scientific & Technical Research 31(1)

Choudhary S, Tiwari M, Poluri KM (2024) A Biorefinery Approach Integrating Lipid and EPS Augmentation Along with Cr (III) Mitigation by *Chlorella minutissima*. Cells 13(24):2047

D'Abzac P, Bordas F, Joussein E, Van Hullebusch ED, Lens PNL, Guibaud G (2012) Metal binding properties of extracellular polymeric substances extracted from anaerobic granular sludges. Environmental Science and Pollution Research *20*(7):4509–4519

Devadasu E, Subramanyam R (2021) Enhanced Lipid Production in *Chlamydomonas reinhardtii* Caused by Severe Iron Deficiency. Frontiers in Plant Science 12:615577

Díaz S, De Francisco P, Olsson S, Aguilera Á, González-Toril E, Martín-González A (2020) Toxicity, Physiological, and Ultrastructural Effects of Arsenic and Cadmium on the Extremophilic Microalga *Chlamydomonas acidophila*. International Journal of Environmental Research and Public Health 17(5):1650

Finnegan PM, Chen W (2012) Arsenic toxicity: the effects on plant metabolism. Frontiers in Physiology 3:182

Ganguly A, Nag S, Bhowmick TK, Gayen K (2024) Phycoremediation of As(III) and Cr(VI) by *Desmodesmus subspicatus*: Impact on growth and biomolecules (carbohydrate, protein, chlorophyll and lipid) — A dual mode investigation. Environmental Science and Pollution Research 31(35):48545–48560

Greipel E, Kósa A, Böddi B, Bakony M, Bernát G, Felföldi T, Preininger É, Kutasi, J (2024) Extraction of chlorophyll a from *Tetradesmus obliquus*—a method upgrade. Biologia Futura 75(2): 243–250

Havlik I, Beutel S, Scheper T, Reardon KF (2022) On-Line monitoring of biological parameters in microalgal bioprocesses using optical methods. Energies 15(3):875

Hofslagare O, Sjöberg S, Samuelsson G (1994) The effect of arsenate and arsenite on photosynthesis in *Scenedesmus obliquus*. A Potentiometric study in a closed CO_2-system. Chemical Speciation and Bioavailability 6(4):95–102

Jiang Y, Purchase D, Jones H, Garelick H (2011) Technical note: Effects of arsenate (AS^{5+}) on growth and production of glutathione (GSH) and phytochelatins (PCS) in *Chlorella vulgaris*. International Journal of Phytoremediation 13(8):834–844.

Kofroňová M, Hrdinová A, Mašková P, Tremlová J, Soudek P, Petrová Š., Pinkas D, Lipavská H (2020) Multi-Component antioxidative system and robust carbohydrate status, the essence of plant arsenic tolerance. Antioxidants 9(4):283

Kramárová Z, Fargašová A, Molnárová M, Bujdoš M (2012) Arsenic and selenium interactive effect on alga *Desmodesmus quadricauda*. Ecotoxicology and Environmental Safety 86:1–6.

Kumar KS, Prasanthkumar S, Ray J (2016) Experimental assessment of productivity, oil-yield and oil-profile of eight different common freshwater-blooming green algae of Kerala. Biocatalysis and Agricultural Biotechnology 8:270–277

Levy JL, Stauber JL, Adams MS, Maher WA, Kirby JK, Jolley DF (2005) Toxicity, biotransformation, and mode of action of arsenic in two freshwater microalgae (*Chlorella* sp. and *Monoraphidium arcuatum*). Environmental Toxicology and Chemistry *24*(10):2630–2639

Lichtenthaler HK (1987) Chlorophyll fluorescence signatures of leaves during the autumnal chlorophyll breakdown. Journal of plant physiology 131(1-2):101-110

Liu W, Wood BA, Raab A, McGrath SP, Zhao F, Feldmann J (2010) Complexation of Arsenite with Phytochelatins Reduces Arsenite Efflux and Translocation from Roots to Shoots in Arabidopsis. PLANT PHYSIOLOGY 152(4):2211–2221

Liu Z, Shen J, Carbrey JM, Mukhopadhyay R, Agre P, Rosen BP (2002) Arsenite transport by mammalian aquaglyceroporins AQP7 and AQP9. Proceedings of the National Academy of Sciences 99(9):6053–6058

Mahlangu D, Mphahlele K, De Paola F, Mthombeni NH (2024) Microalgae-Mediated Biosorption for Effective Heavy Metals Removal from Wastewater: A Review. Water 16(5):718

Mahmod SS, Al-Rajabi MM, Abdul PM, Ding G, Kamarudin KF, Gunny AaN, Tan JP, Takriff MS (2024) Microalgae biomass: A multi-product biorefinery solution for sustainable energy, environmental remediation, and industrial symbiosis. Algal Research 85:103839

Mohanty D (2017) Conventional as well as Emerging Arsenic Removal Technologies—a Critical Review. Water Air & Soil Pollution 228(10)

Murray LA, Raab A, Marr IL, Feldmann J (2003) Biotransformation of arsenate to arsenosugars by *Chlorella vulgaris*. Applied Organometallic Chemistry 7(9):669–674.

Muzaffar S, Khan J, Srivastava R, Gorbatyuk MS, Athar M (2022) Mechanistic understanding of the toxic effects of arsenic and warfare arsenicals on human health and environment. Cell Biology and Toxicology 39(1):85–110

Nowicka B, Nowicka B (2022) Heavy metal–induced stress in eukaryotic algae—mechanisms of heavy metal toxicity and tolerance with particular emphasis on oxidative stress in exposed cells and the role of antioxidant response. Environmental Science and Pollution Research 29(12):16860–16911

Osada K, Maeda Y, Yoshino T, Nojima D, Bowler C, Tanaka T (2017) Enhanced NADPH production in the pentose phosphate pathway accelerates lipid accumulation in the oleaginous diatom *Fistulifera solaris*. Algal Research 23:126–134

Patel A, Tiwari S, Prasad SM (2018) Toxicity assessment of arsenate and arsenite on growth, chlorophyll a fluorescence and antioxidant machinery in *Nostocmuscorum*. Ecotoxicology and Environmental Safety 157:369–379

Piršelová B, Galuščáková Ľ, Lengyelová, L, Kubová V, Jandová V, Hegrová J (2022) Assessment of the Hormetic Effect of Arsenic on Growth and Physiology of Two Cultivars of Maize (*Zea mays* L.). Plants 11(24):3433

Rahman MM, Ng JC, Naidu R (2009) Chronic exposure of arsenic via drinking water and its adverse health impacts on humans. Environmental Geochemistry and Health 31(S1):189–200

Rodríguez-Martín D, Murciano A, Herráiz M, De Francisco P, Amaro F, Gutiérrez JC, Martín-González A, Díaz S (2022) Arsenate and arsenite differential toxicity in *Tetrahymena thermophila*. Journal of Hazardous Materials 431:128532

Shaghaleh H, Hamoud YA, Saleem MH, Elansary HO, Mahmoud EA, Sheteiwy MS (2025) Phytohormonal modulation alleviates arsenic toxicity in rice by enhancing antioxidant defenses, proline metabolism, and arsenic detoxification mechanisms. Scientific Reports 15(1):26953

Shaji E, Santosh M, Sarath K, Prakash P, Deepchand V, Divya B (2020) Arsenic contamination of groundwater: A global synopsis with focus on the Indian Peninsula. Geoscience Frontiers 12(3):101079

Shivaji S, Dronamaraju SVL (2019) *Scenedesmus rotundus* isolated from the petroleum effluent employs alternate mechanisms of tolerance to elevated levels of Cadmium and Zinc. Scientific Reports 9(1):8485

Shrivastav A, Mishra SK, Suh WI, Farooq W, Moon M, Kim T, Kumar K, Choi G, Park MS, Yang J (2015) Characterization of newly isolated oleaginous microalga *Monoraphidium* sp. for lipid production under different conditions. Algal Research 12:289–294

Singh RP, Yadav P, Kumar I, Solanki MK, Roychowdhury R, Kumar A, Gupta RK (2023) Advancement of Abiotic Stresses for Microalgal Lipid Production and Its Bioprospecting into Sustainable Biofuels. Sustainability 15(18):13678

Suarez-Montes D, Borrell YJ, Gonzalez JM, Rico JM (2022) Isolation and identification of microalgal strains with potential as carotenoids producers from a municipal solid waste landfill. The Science of the Total Environment 80: 2149755

Tang WW, Foo SC (2024) Microalgae for freshwater arsenic bioremediation: examining cellular toxicity, bioconcentration factor and eluding an alternative arsenic detoxification pathway. 3 Biotech 14(5):130

Tsuchiya T, Ehara A, Kasahara Y, Hamamura N, Amachi S (2019) Expression of Genes and Proteins Involved in Arsenic Respiration and Resistance in Dissimilatory Arsenate-Reducing *Geobacter*sp. Strain OR-1. Applied and Environmental Microbiology 85(14)

Tyler CR, Allan AM (2014) The effects of arsenic exposure on neurological and cognitive dysfunction in human and rodent studies: a review. Current Environmental Health Reports 1(2):132–147

Upadhyay A, Mandotra S, Kumar N, Singh N, Singh L, Rai U (2016) Augmentation of arsenic enhances lipid yield and defense responses in alga *Nannochloropsis* sp. Bioresource Technology 221:430–437

Villadangos AF, Fu H, Gil JA, Messens J, Rosen BP, Mateos LM (2011) Efflux Permease CgAcr3-1 of *Corynebacterium glutamicum* Is an Arsenite-specific Antiporter. Journal of Biological Chemistry 287(1):723–735

Wang N, Li Y, Deng X, Miao A, Ji R, Yang L (2013) Toxicity and bioaccumulation kinetics of arsenate in two freshwater green algae under different phosphate regimes. Water Research 47(7):2497–2506

Wang Y, Wang S, Xu P, Liu C, Liu M, Wang Y, Wang C, Zhang, C, Ge Y (2015) Review of arsenic speciation, toxicity and metabolism in microalgae. Reviews in Environmental Science and Bio/Technology 14(3):427–451

Xing M, Yan D, Hai M, Zhang Y, Zhang Z, Li F (2024) Arsenic Contamination in Sludge and Sediment and Relationship with Microbial Resistance Genes: Interactions and Remediation. Water 16(24): 3633

Xu H, Wu Q, Wang Y, Zhang Z, Jin C, Zhao Y, Gao M, Guo L (2023) Biomass Accumulation and Physiological Characteristics of *Chlorella pyrenoidosa* with Different Forms of Organic Phosphorus under the Mixotrophic Mode. ACS Sustainable Chemistry & Engineering 12(1):130–140

Yamamura S, Amachi S (2014) Microbiology of inorganic arsenic: From metabolism to bioremediation. Journal of Bioscience and Bioengineering 118(1):1–9

Yang H, Fu H, Lin Y, Rosen BP (2012) Pathways of arsenic uptake and efflux. Current Topics in Membranes 126:325–358

Zhang J, Liu J, Zheng F, Yu M, Shabala S, Song W (2022) Comparative Analysis of Arsenic Transport and Tolerance Mechanisms: Evolution from Prokaryote to Higher Plants. Cells 11(17):2741

Zhang L, Liao C, Yang Y, Wang Y, Ding K, Huo D, Hou C (2019) Response of lipid biosynthesis in *Chlorella pyrenoidosa* to intracellular reactive oxygen species level under stress conditions. Bioresource Technology 287:121414

Zhang W, Dong S, Zhang L, Yu W, Li L, Tsygankov A, Liu J (2025) Effect of nitrogen limitation and carbon sources on hydrogen and lipid production by *Chlorella pyrenoidosa*. Algal Research 91:104128

Declarations

Acknowledgements: The authors sincerely thank Vidyasagar University for providing the necessary facilities and institutional support that enabled the successful completion of this work.

Funding: This research received no external funding.

Author Contribution: Chandan Mandal: Corresponding author, Conceptualization, Methodology, Investigation, Visualization, Writing – original draft, Writing – review & editing. Amal Kumar Mondal: Corresponding author, Investigation, Visualization, Writing – review & editing. Samir Mandi: Methodology, Investigation, Writing – original draft. Prashant Swapnil:

Writing – original draft, Writing – review & editing. All authors read and approved the final manuscript.

Ethical Approval: The authors confirmed that no ethical approval was required since this research study employed only observational techniques that did not involve an intervention with human or animal subjects.

Consent to Participate: The authors confirm that consent to participate is not applicable to this study.

Consent to Publish: The authors confirm that consent to publish is not applicable to this study.

Competing Interests: The authors declare no competing interests.

Data Availability: Yes. I used or generated research data in this study.